Chem Soc Rev

Chemical Society Reviews

rsc.li/chem-soc-rev
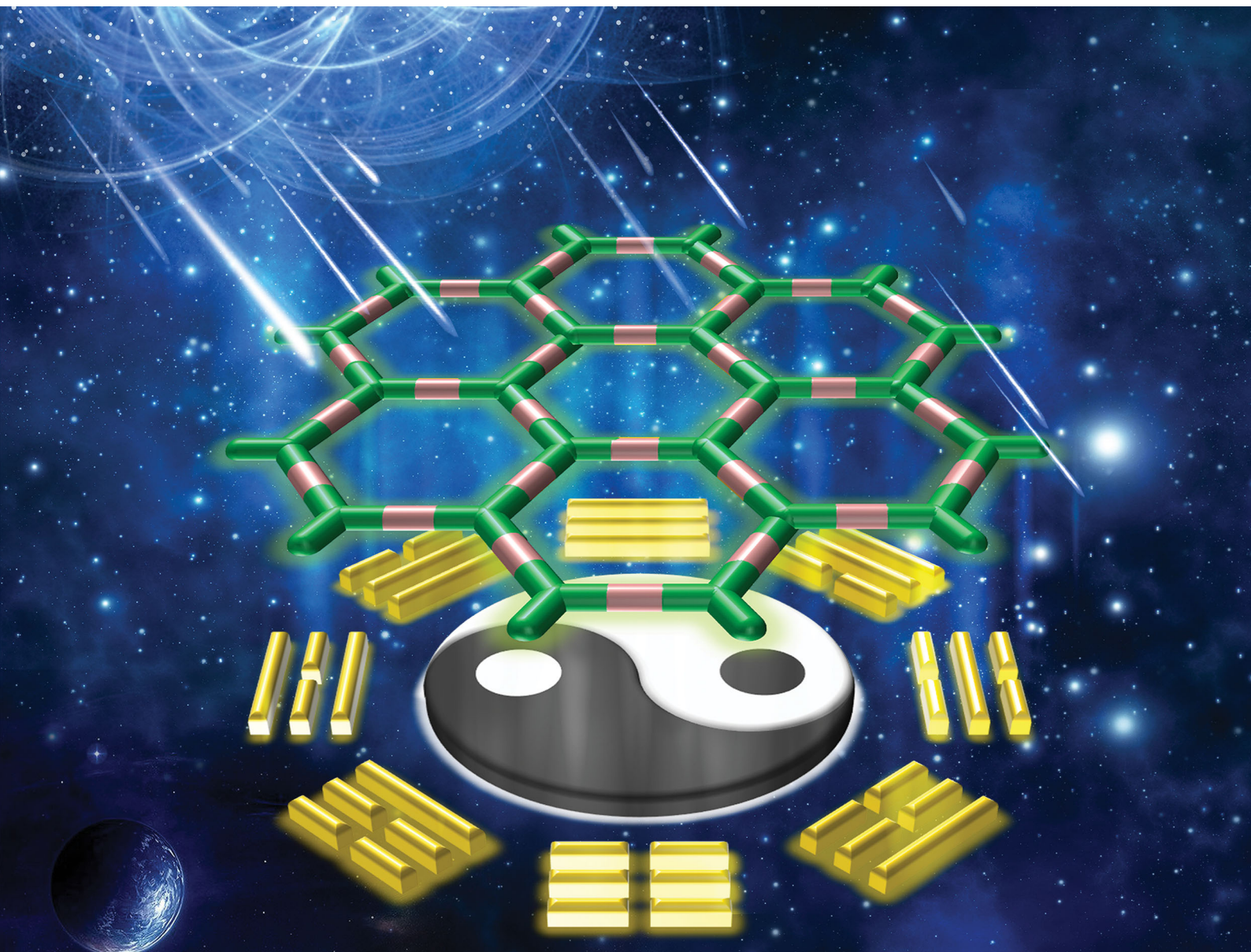
ROYAL SOCIETY
OF CHEMISTRY

TUTORIAL REVIEW
Long Chen *et al.*
New synthetic strategies toward covalent organic
frameworks

Chem Soc Rev

Check for updates

New synthetic strategies toward covalent organic frameworks

Yusen Li,†[a] Weiben Chen,†[a] Guolong Xing,[a] Donglin Jiang [ID][bc] and Long Chen [ID]*[a]

Covalent organic frameworks (COFs) enable precise reticulation of organic building units into extended 2D and 3D open networks using strong covalent bonds to constitute predesignable topologies and tunable pore structures, presenting an emerging class of crystalline porous polymers. Although rapid progress and substantial achievements in COF chemistry over the past 15 years have been realised, highly efficient strategies and reproducible procedures still play a central role in achieving high-quality COFs and serve as a major driving force for the further advancement of this promising field. In this review, we focused on the key progress in synthesising high-quality COF crystallites and films by highlighting their uniqueness from the viewpoints of synthetic strategies and procedures. We discussed representative synthetic methods including mechanochemical synthesis, microwave synthesis, multicomponent reaction, multistep synthesis and linker exchange strategies to compare their features in producing COFs. We scrutinised the recently developed "two-in-one" molecular design strategy to showcase advantages in optimising synthetic conditions such as catalyst, monomer feeding rate and tolerance to functional groups. We analysed interfacial polymerisation for fabricating various COF films by emphasising their scope and applicability. Moreover, we proposed key underlying challenges to be solved and predicted future frontiers from the perspectives of synthesising high quality crystallites and films that are key to practical applications.

Key learning points
1. Key progress in synthesising high-quality COF crystallites and films with their uniqueness from the viewpoints of synthetic strategies and procedures.
2. The synthetic parameters that are detrimental to the crystallinity and porosity of COFs and the optimization methods.
3. A survey and detailed summarization of new synthetic strategies toward COFs like "two-in-one", "double-stage", "linker exchange" and "multicomponent" strategies.
4. Representative advances in new approaches for fabrication of COF films with a focus on interfacial synthesis of single-layer 2D COFs.
5. Key fundamental issues and future directions for synthesising high-quality COFs.

1. Introduction

Designing materials to achieve ordered structures is a central subject of chemistry and materials science. Organising organic materials with predesignable structural orderings has been a challenging target. In this context, covalent organic frameworks (COFs) offer an irreplaceable platform for predesigning organic materials with ordered structures, as they enable topology-guided integration of organic units into crystalline porous polymers to create periodic backbones and built-in pores.[1] Over the past 15 years, COFs have received widespread attention as well as great research enthusiasm to enable rapid progress in design, synthesis and functionalisation, rising as an emerging class of polymers.[1] COFs serve as a promising platform for many applications such as gas adsorption and separation, optoelectronics, drug delivery, heterogeneous catalysis, sensing and energy storage,[1] owing to their multifunctionality originating from their design-ability, topology and unit diversity, porosity and stability.[2] The development of molecular design principles, synthetic strategies and functional explorations has greatly enhanced our capability of designing materials and functions.[3–7]

Most COFs are constructed with strong and dynamic covalent bonds.[1] Recently, more than twenty different linkages have been developed for construction of COFs.[1] Among them, boronic

[a] *Department of Chemistry, Institute of Molecular Plus, and Tianjin Key Laboratory of Molecular Optoelectronic Science, Tianjin University, Tianjin 300072, China. E-mail: long.chen@tju.edu.cn*

[b] *Joint School of National University of Singapore and Tianjin University, International Campus of Tianjin University, Fuzhou 350207, China*

[c] *Department of Chemistry, Faculty of Science, National University of Singapore, Science Drive 3, Singapore 117543, Singapore*

† These authors contributed equally to this work.

esters,[2] triazines,[3] C=C bonds[4,5] and imines[6] are the most widely investigated linkages that enable the synthesis of a diversity of COF families. However, it is still a challenge to synthesise high-quality COF crystallites. One important concern is that polymerisation conditions such as reaction time, temperature, pressure, solvent, catalyst and monomer concentration have various effects on the polymerisation, making the chain crystallisation and propagation very complex.[8] Hence, the synthesis of a new crystalline COF usually requires an exhaustive screening of synthetic conditions, which greatly hampers the development of the COF field.

Despite the difficulty in exploring new strategies for replacing condition screening for polymerisation of monomers into COFs, continuous efforts in this direction bring us new light. In particular, new strategies that are efficient in constructing high-quality COF crystallites and films have been demonstrated, which are distinct in design and synthesis from conventional strategies. These new strategies thus have a high possibility of

opening a new way to develop the chemistry and materials science of COFs. Excellent and comprehensive reviews on the design, synthesis and application of COFs[1,7,9,10] have been available; however, less attention has been paid to these aforementioned new synthetic strategies. To sharpen the topics, this review will focus on scrutinising all synthetic strategies to offer a full picture of the synthetic chemistry of COFs, which provides a new base for considering the most important aspect – how to develop high-quality COF crystallites and films. Firstly, we summarised conventional methods for COF synthesis and showed their use and limitations. Subsequently, we looked at recent advances in exploring unconventional synthetic strategies to construct COFs and compared them with conventional strategies to disclose the clues to new synthetic strategies. Finally, we predicted the key challenges to be addressed and future frontiers from the perspective of synthetic chemistry.

Yusen Li obtained his BSc degree in chemistry from Zhoukou Normal University, China, in 2015. He is currently a PhD candidate under the supervision of Prof. Long Chen at Tianjin University. His research topics mainly focus on the new synthetic approaches and applications of covalent organic frameworks.

Yusen Li

Weiben Chen received his BSc degree in applied chemistry from Tianjin Chengjian University, China, in 2015. He is currently a PhD candidate under the supervision of Prof. Long Chen at Tianjin University. His research focuses on the design and synthesis of functional covalent organic frameworks for photocatalysis.

Weiben Chen

Guolong Xing received his BSc degree in chemistry from Jilin University in 2012 and his PhD degree in macromolecular chemistry and physics from Jilin University under the supervision of Prof. Teng Ben in 2018. He then joined Prof. Long Chen's group as a lecturer at Tianjin University. His current scientific interests focus on the design and synthesis of novel porous materials.

Guolong Xing

Donglin Jiang received his BSc degree (1989) from Zhejiang University and his PhD degree (1998) from The University of Tokyo. In 1998, he took an assistant professorship (1998–2000) at The University of Tokyo and in 2000 he was appointed the group leader of the AIDA Nanospace Project, Exploratory Research for Advanced Technology (ERATO), Japan Science and Technology Agency (JST). In 2005, he moved to the Institute for

Donglin Jiang

Molecular Science (IMS), National Institutes of Nature Sciences (NINS), as an associate professor and took a concurrent associate professorship at SOKENDAI, Japan. In January 2016, he moved as a full professor to the Japan Advanced Institute of Science and Technology. In 2018, he was appointed as a professor at National University of Singapore.

2. Conventional synthetic methods

In general, most reported COFs have been synthesised in a sealed vessel under solvothermal conditions. However, during the synthetic process, many factors play significant roles in the crystallinity of COFs: for instance, the pressure in the sealed vessel, temperature, reaction time, the volume ratio of solvent combinations and the amount of catalyst (Fig. 1). In order to obtain high-quality COFs, tremendous work and efforts have to be devoted to finding optimal reaction conditions (especially the screening of solvents), which greatly hinders the development of COFs. On the other hand, even when the optimised conditions are fixed, there are huge batch-to-batch variations between the COF samples due to the sensitivity of COF quality to synthetic conditions. Thus, exploring new synthetic strategies for preparation of high-quality COFs with reproducibility is highly desired and challenging.

Covalent triazine frameworks (CTFs) are a special class of COFs linked by triazine rings. Ionothermal synthesis is one of the most widely used methods for the preparation of CTFs instead of the solvothermal method. However, the resulting polymers usually have poor crystallinity or are even amorphous.[3] Additionally, harsh reaction conditions (e.g., high reaction temperature and long reaction time) are unavoidable in the ionothermal procedure, which may cause partial carbonisation. Meanwhile, metallic residues may exist from the molten metal salts, leading to an unsatisfactory performance as well as poor structure–property correlations. Therefore, it is highly desirable to develop new synthetic strategies to achieve pure crystallites with improved crystallinity under mild conditions, which is crucial for the future development of CTFs.

COF films have attracted much attention owing to their promising applications in molecular sieving and separation, electronic devices, chemical sensors and photocatalysts.[9] However, the difficulties in the fabrication of high-quality COF films greatly impede their practical applications. For example, a method of *in situ* growth of 2D COF films on single-layer graphene under solvothermal conditions has been explored.[11] The resulting COF films on graphene possess domain structures
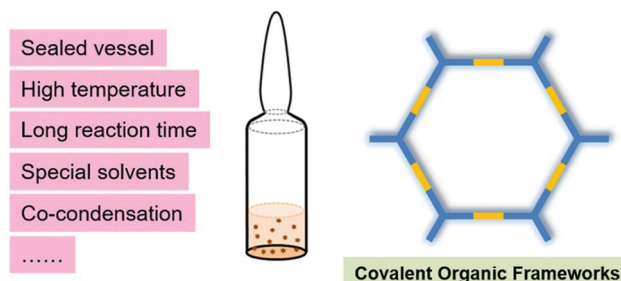

Fig. 1 Representative condition metrics of conventional solvothermal and ionothermal syntheses of crystalline COFs.

and hardly afford smooth surfaces for direct applications. The as-prepared COF films rely on specific supports and cannot be further transferred to desired substrates for characterisation and specific application. In addition, the yield of film formation is low because the major product is COF powders in a solution phase. Apart from that, controlling the thickness of COF films under solvothermal conditions is also challenging. Hence, it is imperative to develop new synthetic strategies to properly address these issues.

From the perspectives of synthetic strategies and conditions, the quality of COF crystallites and films is affected by many parameters. In the following section, we summarise the recent representative advances in developing new strategies to synthesise COFs.

3. New synthetic strategies

3.1 Microwave and mechanical syntheses

It is well known that microwave irradiation provides an effective way for the synthesis of organic polymers and metal organic frameworks (MOFs). The microwave synthesis method was first employed to prepare crystalline boron-based two-dimensional COF-5 and three-dimensional COF-102 in 2009.[12] The resulting COFs exhibited comparable or even higher surface areas (2019 $m^2 g^{-1}$ for COF-5 and 2926 $m^2 g^{-1}$ for COF-102) than those obtained *via* the conventional solvothermal method (1590 $m^2 g^{-1}$ for COF-5 and 3472 $m^2 g^{-1}$ for COF-102) while greatly shortening the reaction time. Only after irradiation for 20 min, highly crystalline COF-5 and COF-102 were readily obtained (Fig. 2a–c). The reaction rate is about 200 times higher than that of the solvothermal synthesis.

Mechanochemical (MC) synthesis is a simple yet cost-effective method which has been applied for MOF synthesis and it has also been demonstrated to be applicable to the synthesis of COFs. Three thermally and chemically stable COFs [TpPa-1 (MC), TpPa-2 (MC), and TpBD (MC)] were successfully constructed by solvent-free mechanical grinding at room temperature in a short time (40 min).[13] The proceeding of the mechanical force induced reaction can be easily recognised by the colour change of the powder upon grinding (Fig. 2d). Although these mechanically synthesised COFs showcased limited crystallinity and porosity, this strategy did feature merits such as eco-friendliness, easy

Long Chen received his PhD degree in 2009 under the supervision of Prof. Donglin Jiang at the Institute for Molecular Science (IMS, Japan). He then joined Prof. Klaus Müllen's group at the Max Planck Institute for Polymer Research (MPIP, Germany) as an Alexander von Humboldt research fellow. In March 2012, he was appointed a project leader in the same group. In September 2014, he was appointed as a professor at Tianjin University. His current research focuses on the design and synthesis of 2D conjugated porous polymers for catalysis and energy conversion.

Long Chen
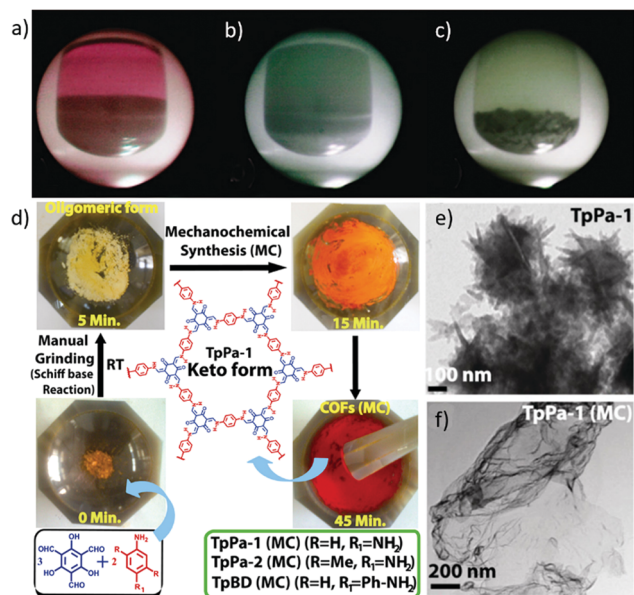
Fig. 2 (a–c) Digital camera images recorded from the observation port of a microwave reactor showing COF-5 reaction and purification: (a) gray-purple COF-5 powder formed after the initial synthesis; (b) removal of trapped HHTP oxidation impurities by a microwave extraction process (acetone); and (c) second microwave extraction results in purified gray COF-5 powder (S_{BET} = 2019 m^2 g^{-1}). Reproduced with permission from ref. 12. Copyright 2009, American Chemical Society. (d) Schematic representation of the MC synthesis of TpPa-1 (MC), TpPa-2 (MC), and TpBD (MC) through simple Schiff base reactions performed by MC grinding using a mortar and pestle. (e and f) High-resolution TEM images of TpPa-1 and TpPa-1 (MC). Reproduced with permission from ref. 13. Copyright 2013, American Chemical Society.

operation and feasibility for scale up synthesis. The obtained COFs tended to exhibit sheet-like structures probably due to the exfoliation of the 2D layers during the grinding process reminiscent of the delamination process of graphite, while the TpPa-1 prepared by the solvothermal method exhibited a flower-like morphology (Fig. 2e and f). In addition, two sulfonated COFs (NUS-9 and NUS-10) exhibiting high intrinsic proton conductivity were synthesised by a similar liquid-assisted grinding method.[14] It is noteworthy that NUS-10 could not be directly synthesised by the conventional solvothermal approach owing to the poor solubility of 2,5-diaminobenzene-1,4-disulfonic acid in organic solvents. This result indicates that mechanical synthesis may provide an alternative to preparing COFs from highly polar monomers.

Microwave and mechanochemical syntheses possess advantages of short reaction times, high yields and possibilities for large-scale production. These methods might make unique contributions to the future development of COF materials.

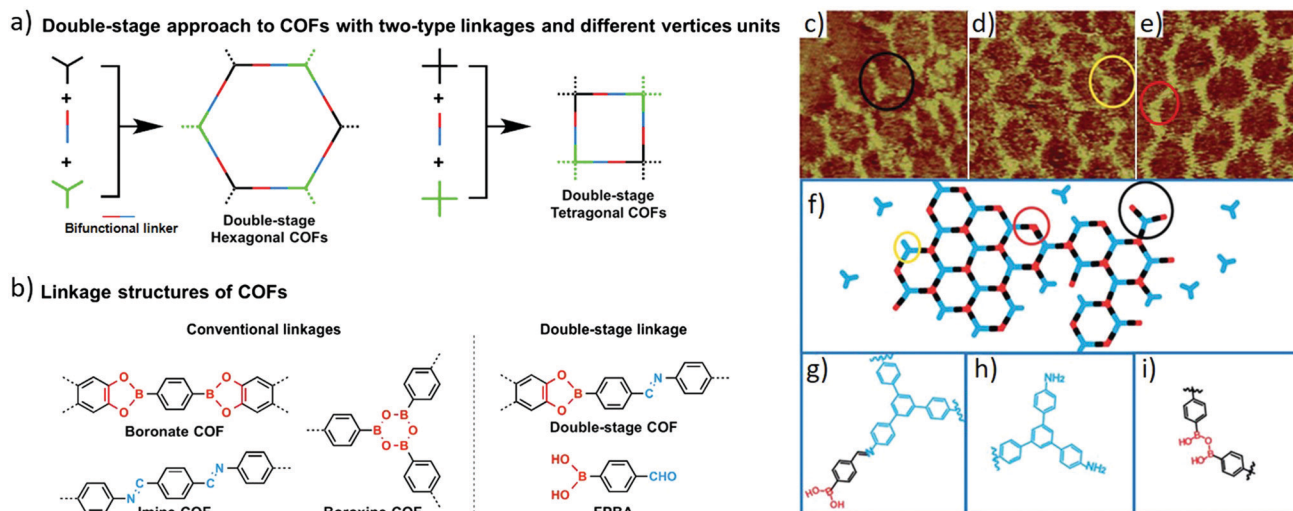### 3.2 Multicomponent reaction (MCR) and multistep synthesis (MSS) strategies

COFs are generally synthesised by co-condensation of one linker and one knot, which is the conventional [1+1] two-component approach. This [1+1] two-component approach is inefficient at increasing the multiformity of skeletons unless novel linkers or

knots are used. Accordingly, a multiple-component reaction (MCR) strategy emerged, realising the utilisation of more than two kinds of building blocks to construct crystalline COFs with much enhanced structural diversity. Besides, the multiple-step synthesis (MSS) approach is also employed to synthesise COFs with novel linkages.

Orthogonal reaction is a typical multicomponent reaction strategy which has been widely applied in biochemistry and supramolecular chemistry, and this strategy has also been applied in the preparation of COFs in recent years. Hexagonal NTU-COF-1 and NTU-COF-2 were representative COFs constructed by orthogonal reaction which exhibited two different kinds of reversible covalent linkages (*i.e.* boroxine and imine).[15] The prerequisite to form two types of reversible covalent bonds is that at least one of the building blocks must consist of two different functional groups. Even though binary NTU-COF-1 and ternary NTU-COF-2 exhibited intense PXRD peaks, NTU-COF-1 only exhibited a low surface area (41 m^2 g^{-1}) probably due to channel plugging, while NTU-COF-2 featured a large surface area of 1619 m^2 g^{-1}. Interestingly, these two crystalline COFs cannot be synthesised by a stepwise method because the formations of imine linkages and a B$_3$O$_3$ ring or a C$_2$B$_2$O ring were in parallel, which was detected by high performance liquid chromatography (HPLC).

Certainly, COFs with various topologies and different pore sizes can also be obtained *via* a double-stage approach,[16] which is another representative orthogonal reaction strategy. The result indicated that boronate–hydrazone double linkages could also be formed to construct crystalline double-stage COFs besides boronate–imine and boroxine–imine linkages (Fig. 3a). One of the building blocks containing an aldehyde and boronic acid, such as 4-formylphenylboric acid (FPBA, Fig. 3b), is the premise to simultaneously form two different types of linkages. Various topological structures from hexagonal to tetragonal and rhombus frameworks can be constructed by varying the symmetry of the monomers. It is noteworthy that the obtained double-stage COFs not only possess complex compositions, but also exhibit excellent crystallinity, large surface areas (557–1975 m^2 g^{-1}) and tunable band gaps (1.29–2.34 eV).

Interestingly, this orthogonal strategy not only works well in a liquid phase but is also applicable for on-surface synthesis. Single-layered imine–boroxine hybrid single-layered covalent organic frameworks (sCOFs) were constructed on the surface of highly oriented pyrolytic graphite (HOPG) *via* a gas/solid interface reaction.[17] The synthetic procedure was briefly described as follows: the amine monomer of 1,3,5-tris(4-aminophenyl)benzene (TAPB) was deposited on HOPG, then the loaded HPOG was placed in a reactor with the bifunctional monomers bearing both boronic acid and aldehyde functional groups and CuSO$_4$·5H$_2$O powder. After that, the reactor was closed and heated at 120 °C for 3 h. The resulting sCOFs were directly characterised by scanning tunnelling microscopy (STM) (Fig. 3c). Interestingly, when the asymmetrical bifunctional monomer 3-formylphenylboronic acid (3FPBA) was used, the windmill structures exhibited surface chirality which had never been reported before. Besides, the formation of imine bonds and boroxine rings can be intuitively observed

This journal is © The Royal Society of Chemistry 2020

Chem. Soc. Rev., 2020, **49**, 2852–2868 | **2855**

Fig. 3 (a) Schematic representation of the double-stage approach to COFs with bifunctional linkers made of three different building blocks. (b) Typical linkage structures of boronate, boroxine and imine COFs, and linkage structure of the double-stage COF along with the structure of the bifunctional linker 4-formylphenylboronic acid (FPBA). Reproduced with permission from ref. 16. Copyright 2015, Springer Nature. (c–e) STM images (10 × 10 nm²) of the boundaries of sCOFA. (c) The long trefoil structure, outlined by a black ring. (d) The short trefoil structure highlighted by a yellow ring. (e) The zig-zag structure shown by a red ring. (f) Structural models for the boundaries of sCOFA. (g) Chemical structure for the long trefoil structure. (h) Chemical structure for the short trefoil structure. (i) Chemical structure for the zig-zag structure. Reproduced with permission from ref. 17. Copyright 2017, Royal Society of Chemistry.

in the STM images (Fig. 3c–e) which was consistent with previously reported results.[15]

The multicomponent condensation strategy is appropriate for constructing COFs with a unitary type of linkage such as boronate[18] or imine.[19] The synthetic process of these multi-component COFs is similar to the traditional [1+1] approach. The molar ratio of two functional groups must be appropriate (*i.e.* the ratio of the formyl to amino groups is 1 : 1, while the ratio of hydroxyl to boronic acid is 2 : 1) and a suitable stoichiometry of linkers is required to form closed hexagons or tetragons. 53 different boronate COFs were successfully synthesised by condensing one knot with two or three linkers to afford hexagonal or tetragonal COFs (Fig. 4).[18] Interestingly, the organic monomers were asymmetrically distributed in the multicomponent COFs so that anisotropic skeletons and unusually shaped pores were formed. Two other imine linked multi-component COFs (SIOC-COF-1 and SIOC-COF-2) bearing three different kinds of pores were also realized by this strategy.[19] These two triple-pore COFs were prepared by condensation of 4,4′,4″,4‴-(ethene-1,1,2,2-tetrayl)tetraaniline (ETTA) and two dialdehydes with varied lengths, which further indicated the universality of the multicomponent strategy.

Very recently, a series of imidazole-linked ultrastable COFs have been prepared *via* the reversible/irreversible Debus–Rad-ziszewski multicomponent reaction strategy (Fig. 5).[20] The robust imidazole COFs were obtained by one-pot covalent assembly and condensation of diketones, ammonia, and aldehydes (the molar ratio is 1.5 : 9 : 1) in acetic acid under reflux while five covalent bonds were newly formed in each imidazole ring. These imidazole-linked COFs exhibited outstanding chemical stabilities in common solvents and even under harsh conditions such as 9 M NaOH and 9 M HCl. Moreover, these robust COFs feature
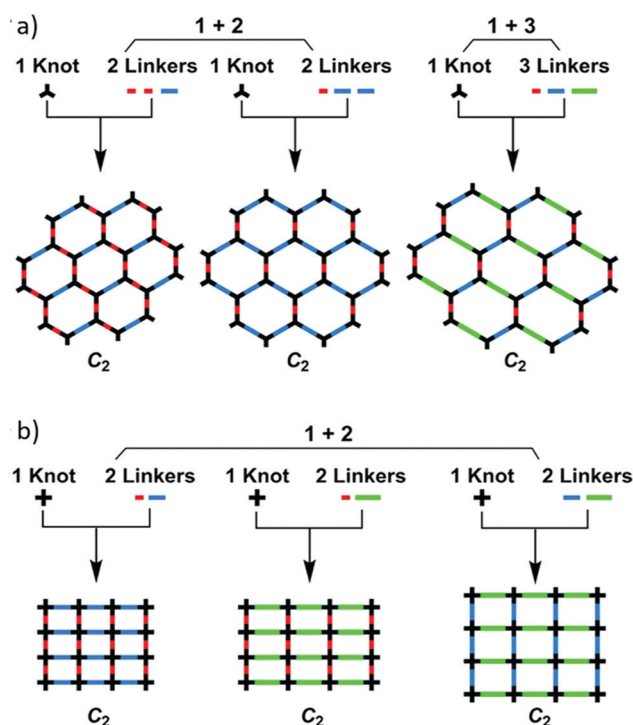
Fig. 4 Multicomponent strategy for the synthesis of hexagonal and tetragonal multicomponent COFs with unitary linkage. Reproduced with permission from ref. 18. Copyright 2016, Springer Nature.

satisfactory crystallinities and high surface areas (506–815 m² g⁻¹). Therefore, this work has set a new level for precise covalent assembly of monomers to prepare COFs *via* reversible/irreversible multicomponent reactions, which opens a new way to construct robust COFs with increased structural complexity.
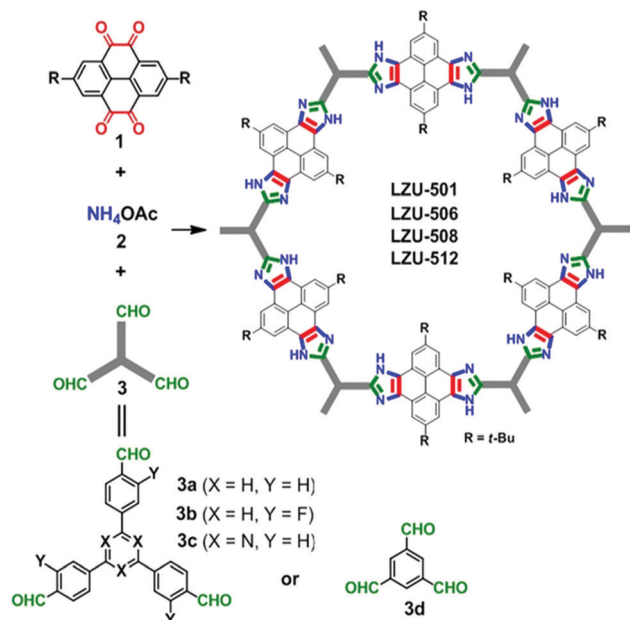
Fig. 5 One-pot synthesis of imidazole-linked COFs by the *in situ* formation of five-membered cyclic linkages. Reproduced with permission from ref. 20. Copyright 2019, American Chemical Society.

The cascade reaction approach is another effective means to construct ultrastable COFs with robust cyclic linkages (Fig. 6).[21] A series of benzoxazole-based COFs were synthesised by cascade reactions of 2,5-diamino-1,4-benzenediol dihydrochloride with different aldehydes. Highly crystalline benzoxazole-based COFs with large surface areas (706–1305 m^2 g^{-1}) were obtained by heating the monomers in a mixture of *N*-methyl-2-pyrrolidone (NMP) and mesitylene (1/1, v/v) with benzimidazole as an additive at 185 °C for 5 days. The benzoxazole linkage endows the

frameworks with superior stability in strong acid and base and under irradiation with visible light. The benzoxazole-based COFs were demonstrated as photocatalysts for oxidative hydroxylation of arylboronic acids to form phenols upon visible light irradiation.

Besides the one-pot cascade reaction to afford robust cyclic structure linked COFs, post-modification is another efficient method for construction of robust COFs. For instance, the Povarov (aza-Diels–Alder) reaction was employed to transform imine-linked COFs into quinoline-linked COFs.[22] The quinolone rings were formed by the cycloaddition of aryl imines and arylalkynes. Although the conversion of imines to quinolines (Fig. 7a) is about 25–30% as determined by X-ray photoelectron spectroscopy (XPS) analyses, the stabilities of the frameworks towards strong acid, strong base and redox reagents were dramatically enhanced. Additionally, crystalline cyclic carbamate and thiocarbamate-linked frameworks were prepared *via* a multi-step post-modification method.[23] A three-step solid-state synthetic process was involved in the transformation of imines to carbamates, which induced significant structural changes in each step (Fig. 7b). The transformation efficiencies were accurately evaluated by ^{15}N cross polarisation magic angle spinning
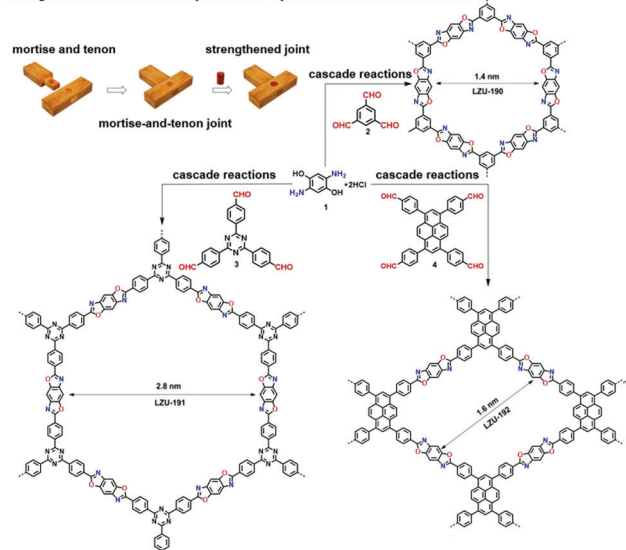

Fig. 6 One-pot synthesis of benzoxazole-linked COFs (LZU-190, LZU-191, and LZU-192) *via* cascade reactions. Reproduced with permission from ref. 21. Copyright 2018, American Chemical Society.
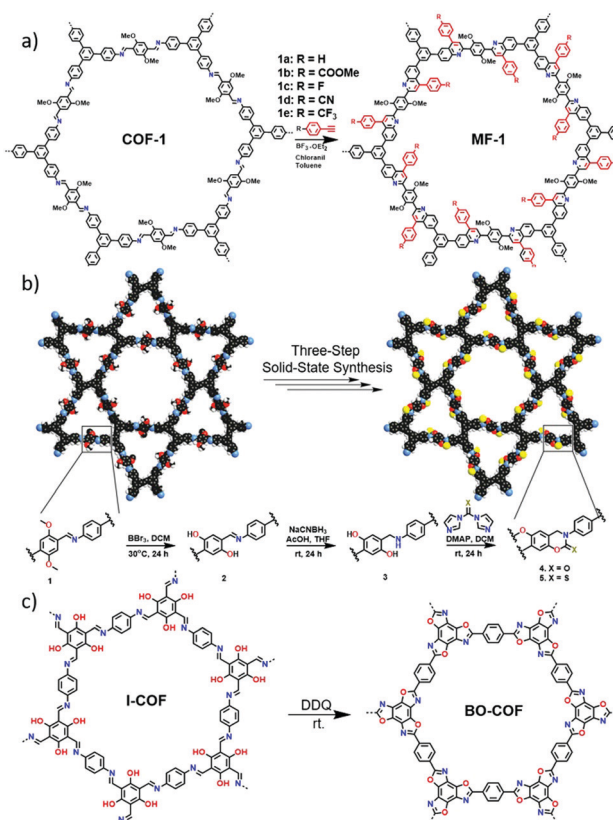

Fig. 7 (a) Post-synthetic modification of COFs *via* the aza-Diels–Alder reaction. Reproduced with permission from ref. 22. Copyright 2018, Springer Nature. (b) Synthesis of cyclic carbamate and thiocarbamate-linked COFs by a three-step solid-state synthesis process. Reproduced with permission from ref. 23. Copyright 2019, American Chemical Society. (c) The oxidative cyclization of I-COF into BO-COF. Reproduced with permission from ref. 24. Copyright 2019, American Chemical Society.

This journal is © The Royal Society of Chemistry 2020

Chem. Soc. Rev., 2020, **49**, 2852–2868 | **2857**

(CP-MAS) NMR spectroscopy, revealing an overall yield from 72% to 86%. Notably, the benzoxazole-linked COF (BO-COF) has been demonstrated to be alternatively synthesised *via* the oxidative cyclization of the corresponding imine-linked COF (Fig. 7c).[24] Very recently, quinoline-linked COFs have also been constructed *via* three-component one-pot Povarov reactions and another α-aminonitrile-linked COF was synthesised by the one-pot multicomponent Strecker reaction as well.[25]

Multicomponent reaction and multistep synthetic strategies can be used to construct COFs with enhanced complexity and unique properties which cannot be obtained by the conventional methods. Note that these methods are effective in developing robust linkages and increasing the diversity of COFs.

3.3 Variation of catalysts

Most imine-linked COFs have been synthesised in the presence of aqueous acetic acid (AcOH) as a catalyst. However, the acidic conditions are incompatible with components in some specific cases.

Basic pyrrolidine was utilized as the catalyst to realise the conversion of amorphous polyimine to a crystalline COF (TpBD) (Fig. 8a).[26] The amorphous polyimine was formed by refluxing benzidine (BD) and 1,3,5-triformylphloroglucinol (Tp) in tetrahydrofuran (THF) for 2 h and this oligomer underwent amorphous-to-crystalline transformation to afford a crystalline TpBD COF. As acidic catalysts might etch the Fe_3O_4 template, which is detrimental to the formation of core–shell structures, alkaline pyrrolidine was developed as the catalyst to promote the amorphous-to-crystalline transformation. These results demonstrated that the basic pyrrolidine not only exerted no influence on the inorganic template but also dramatically

increased the surface area of the TpBD COF (1883 m^2 g^{-1}), which is apparently higher than that of the COF obtained *via* the conventional acid-catalysis method (680 m^2 g^{-1}).

On the other hand, Lewis acidic metal triflates were also employed as catalysts for imine-linked COF formation at low temperature (Fig. 8b).[27] Metal triflates could significantly improve the rate of imine formation and exchange even at an extremely low catalyst loading (0.0001 equiv. per aniline). Among these metal triflate catalysts, $Sc(OTf)_3$ shows the best catalytic activity due to the smallest ionic radius of Sc(III) compared to the other metal triflates. The TAPB–PDA COF with an ultrahigh surface area (2175 m^2 g^{-1}) was obtained when 0.02 equiv. of $Sc(OTf)_3$ was used for the reaction at room temperature in only 10 min. This surface area is much larger than that of the previously reported TABP–PDA COF ($\sim$600 m^2 g^{-1}) synthesized under AcOH catalysis. However, a further increment of $Sc(OTf)_3$ to 0.06 or 0.1 equiv. only afforded a TAPB–PDA COF with moderate crystallinity as revealed by broadened PXRD peaks, which indicate that excess catalyst inhibits the imine exchange process. Furthermore, another two hexagonal 2D imine-linked COFs were constructed by this approach, demonstrating the generality and tolerance of this metal triflate catalysed polymerisation.[27]

Subsequently, a novel salt-mediated crystallisation approach was proposed to synthesise diverse high-quality COFs.[28] *p*-Toluenesulfonic acid (PTSA–H_2O) was introduced as a molecular organiser to induce reversibility and repair defects in the networks of COFs. High quality COFs with satisfactory crystallinity and surface areas (as high as 3000 m^2 g^{-1}) were obtained *via* a facile process: PTSA and diamines were adequately mixed; 1,3,5-triformylphloroglucinol (Tp) and few amounts of water were added into the mixture in sequence. The mixture was further heated at 170 °C
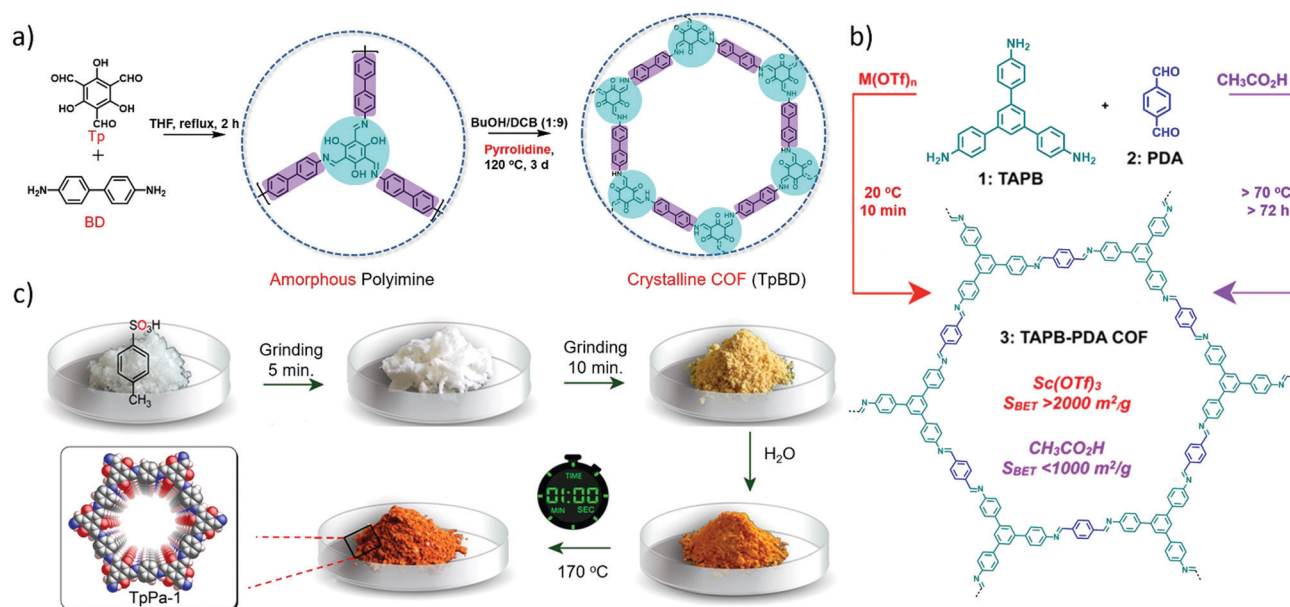
Fig. 8 (a) The amorphous-to-crystalline conversion process catalysed by pyrrolidine. Reproduced with permission from ref. 26. Copyright 2016, Wiley-VCH. (b) Comparison of the synthesis of TAPB–PDA COF from TAPB and PDA using conventional CH_3CO_2H-catalyzed and newly developed M(OTf)$_3$-catalysed conditions. Reproduced with permission from ref. 27. Copyright 2017, American Chemical Society. (c) Synthesis of COFs *via* a molecular organization approach. Reproduced with permission from ref. 28. Copyright 2017, American Chemical Society.

2858 | *Chem. Soc. Rev.*, 2020, **49**, 2852–2868

This journal is © The Royal Society of Chemistry 2020

for 60 s after thoroughly mixing (Fig. 8c). During the formation of the COF, PTSA plays two roles: one is the catalyst and the other is the acid reactant for the formation of PTSA–amine salts which can function as templates for regulating the crystallisation of the 2D COFs by hydrogen-bonding interaction. Large scale ($\sim$10 g h^{-1}) synthesis of COFs could be realised upon using a twin-screw extruder and various kinds of shapes can be facilely gained by imitating the ancient terracotta process. Those materials exhibited outstanding hydrolytic stabilities and remarkable reversible water adsorption capacities so that they can serve as suitable candidates for dehumidification. Besides, a series of acid–diamine salts were utilised as primary reactants to synthesise COFs and the effects of hydrogen-bonding distance in acid–diamine salts on the crystallinity as well as porosity of the COFs were investigated in detail.[29] It is demonstrated that a moderate hydrogen bonding distance of about 2.06–2.19 Å was beneficial to constructing COFs with enhanced crystallinity and porosity.

The development of these novel catalysts is able to address some limitations of aqueous AcOH catalyst, and modulate the rates of imine formation and exchange processes, thereby improving both the crystallinity and porosity of the resulting COFs.

3.4 Linker-exchange strategy

Self-correction and linker-exchange protocols are developed on reversible covalent bonds under thermodynamic equilibrium for achieving crystalline and stable structures. The COF to COF transformation was realized through the linker-exchange strategy at a solid–solution interface.[30] Qian et al. found that

TP–COF–DAB exhibits higher crystallinity and thermal stability than TP–COF–BZ due to the higher activity of 1,4-diamino-benzene (DAB) than that of benzidine (BZ). Inspired by these results, the authors successfully demonstrated that TP–COF–BZ could be converted to TP–COF–DAB with free 1,4-diaminobenzene in a sealed glass tube at 120 °C in 3 days. The in situ COF-to-COF transformation provides a new way for post-synthetic functionalisation of COFs by structural doping (Fig. 9a).

It is highly interesting to realise the transformation of amorphous covalent organic polymers (COPs) into highly crystalline COFs by a linker exchange approach based on reversible covalent linkages. Recently, linker transformation from amorphous covalent organic polymers (COPs) to COFs has been explored by employing diverse linkages under different types of solvothermal conditions (Fig. 9b).[31] Surprisingly, the linkers of amorphous imine-linked COPs were easily replaced by 1,4,5,8-naphthalenetetracarboxylic anhydride (L^1) or pyromellitic dianhydride (L^2), converting into imide-linked COFs with high crystallinity and porosity. In contrast, the linkage replacement of imide-linked COPs with 1,4-terephthalaldehyde is unsuccessful. Zhai et al. attributed these results to the higher stability of imide linkages and the lack of functional groups for 1,4-terephthalaldehyde to form energy-favoured products. However, when the replacing linkers were modified with two additional OH groups, imine-linked COPs can be successfully converted to highly crystalline imide-linked COFs owing to the additional noncovalent interactions of H-bonding.

Recently, a series of large single crystals of imine-linked 3D COFs were obtained under the modulation of aniline which is a
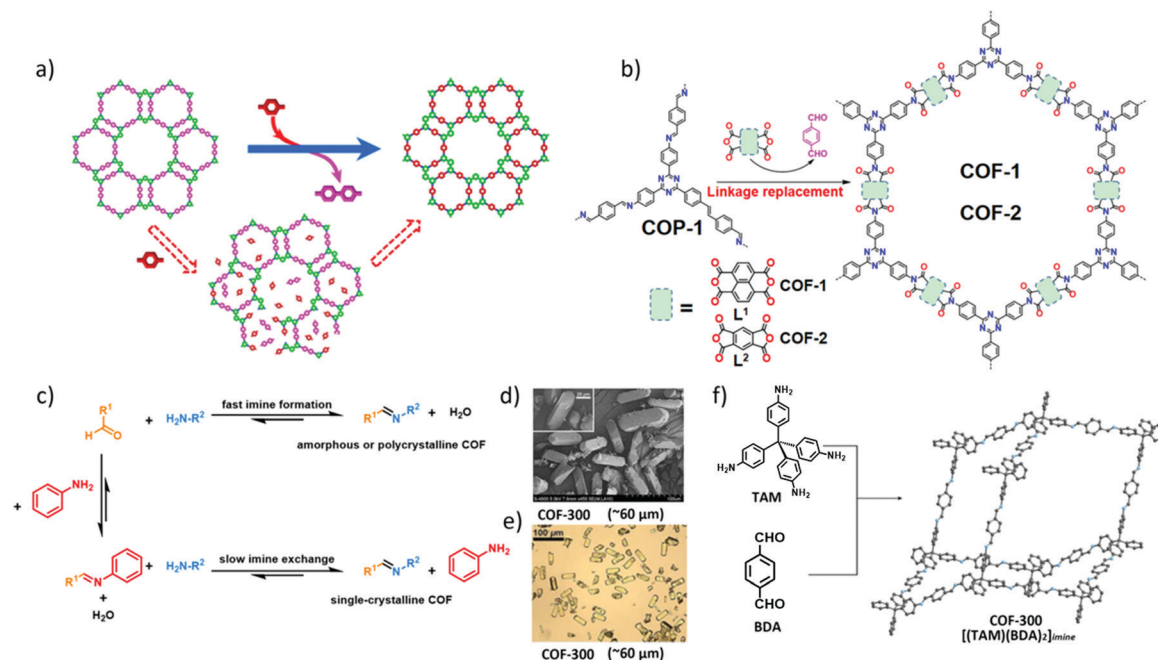
Fig. 9 (a) Proposed process for the in situ transformation of TP–COF–BZ into TP–COF–DAB in the presence of 1,4-diaminobenzene. Reproduced with permission from ref. 30. Copyright 2017, American Chemical Society. (b) Conversion of amorphous COP-1 to COFs using the linker-exchange strategy. Reproduced with permission from ref. 31. Copyright 2019, Wiley-VCH. (c) The scheme of crystal growth of large imine-based COFs modulated by aniline. (d and e) Scanning electron microscopy (SEM) and optical microscopy images of single-crystalline COF-300. (f) Imine condensation between TAM and BDA produced single-crystalline COF-300. Reproduced with permission from ref. 6. Copyright 2018, American Association for the Advancement of Science.

This journal is © The Royal Society of Chemistry 2020

Chem. Soc. Rev., 2020, 49, 2852–2868 | 2859

breakthrough in the synthesis of 3D COFs.[6] Large excesses of aniline as a modulator and a nucleation inhibitor were added to the reaction systems for improving the reversibility of imine formation and disruption of the imine exchange process (Fig. 9c).[6] The size of single crystal COF-300 could reach up to 100 μm in the presence of a large excess of aniline modulator (15 equiv.) in 30 to 40 days (Fig. 9d and e). More importantly, the single crystal structure of COF-300 was first resolved with the sevenfold interpenetration and refined at a resolution of 0.83 Å by collecting single-crystal X-ray diffraction data (Fig. 9f). Additionally, the generality of the method was confirmed by growth of three other single crystals of LZU-79, LZU-111, and COF-303.

Both the monofunctional aldehyde (I, Fig. 10a) and amine (II, Fig. 10a) can be used as the competitors to regulate the formation of Schiff-base COFs.[32] When 12 equivalents of I and II were introduced into a reaction system of 1,3,5-benzenetri-carbaldehyde (BTCA) and 1,3,5-tris(4-aminophenyl)benzene (TAPB), the polycondensation reactions of BTCA and TAPB significantly slowed down. Accordingly, the resulting COF exhibited sharper diffraction peaks and larger surface area ($882 \ m^2 \ g^{-1}$) than the counterpart synthesised without addition of competitors ($432 \ m^2 \ g^{-1}$). The morphology can be controlled by the mono-mer concentrations and solvent compositions (Fig. 10b and c), while uniform COF films can be facilely fabricated at the water–oil interface or substrates such as copper foil (Fig. 10d). The films on HOPG function as gas sensors with good sensitivity and repeatability *via* reversible colour changes from red-purple to cyan.

The linker-exchange strategy can significantly enhance the reversibility of COF formation and accordingly reduce the kinetic traps; thus highly crystalline COFs can be smoothly obtained. Furthermore, this strategy is conducive to the formation of COF materials with regular structures and morphologies.
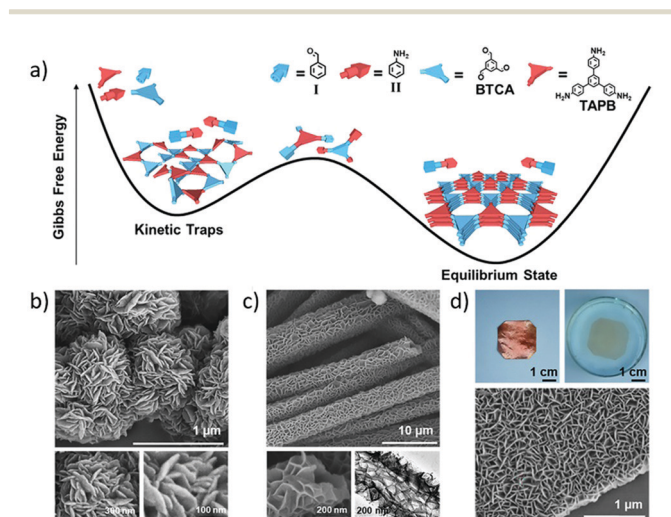
3.5 Control over the monomer feeding rate

As mentioned above, introduction of a large excess of aniline plays vital roles in modulating the nucleation and growth rates to produce high quality COF crystallites. On the other hand, controlling the monomer feeding rate is also an effective way of modulating the nucleation–elongation process of COF for-mation. The nucleation and growth of COFs have been studied in detail by controlling the feeding rate of monomers (Fig. 11).[33] It was revealed that the nucleation–growth process of the 2D boronate ester COFs can be broken by crystallite aggregation and precipitation. On the other hand, the addition of enough amount (80% volume percentage) of CH_3CN as the co-solvent can significantly inhibit the precipitation, and thus produce stable colloidal suspensions of crystalline 2D COF nanoparticles. Fresh monomers were slowly introduced into the stable colloidal suspensions for preventing the fast nucleation process, resulting in isolated crystals in micrometer sizes (Fig. 11a). This process was clearly monitored by exciton diffusion studies (Fig. 11b and c), where smaller COF crystallites more easily underwent exciton–exciton annihilation. In contrast, the faster addition rate of mono-mers led to the exceeding of a critical nucleation concentration, and the reaction was dominated by the generation of new particles.

Besides, highly ordered CTFs were also successfully obtained upon slow addition of the monomers under mild conditions, overcoming the difficulties and disadvantages that originated from the conventional ionothermal method. A new alternative condensation reaction of aldehydes with amidine dihydrochloride was applied instead of the conventional trimerization of aromatic nitriles; thus the feeding rate of aldehyde monomers was tuned to control the nucleation process in an open system (Fig. 12).[34] The full width at half maximum (FWHM) of the dominant diffraction

Fig. 10 (a) Gibbs free energies of reaction systems in different states; (b and c) field-emission scanning electron microscopy (FE-SEM) images of COFs with different morphologies; (d) digital photos of films growing on copper foil and floating on water, and its FE-SEM image (bottom). Reproduced with permission from ref. 32. Copyright 2019, Elsevier.
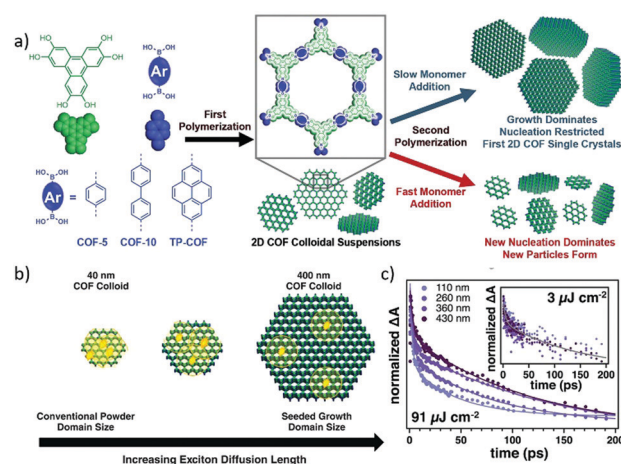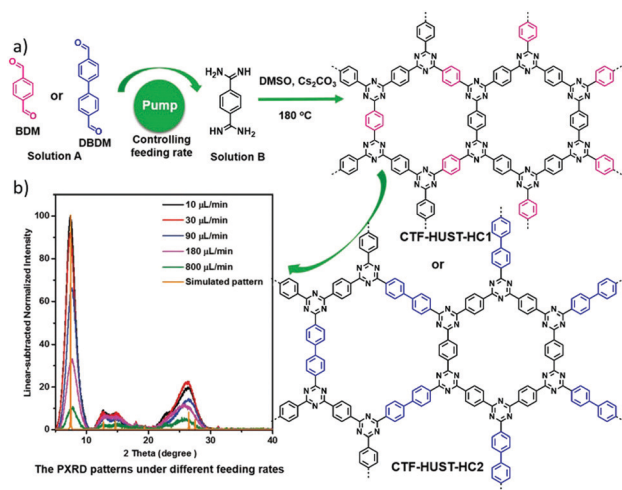

Fig. 11 (a) Schematic illustration of controlled 2D polymerization through a two-step seeded growth approach. (b) Depiction of exciton distribution in COF-5 single crystals of different sizes. Exciton interactions at boundaries are highlighted. (c) Exciton decay kinetics (dots) and fits (lines) of COF-5 colloids of different sizes at high photon fluence (91 mJ per pulse) observed at 410 nm. Inset: Exciton decay kinetics (dots) and fit (line) at low photon fluence (3 mJ per pulse) observed at 410 nm. Reproduced with permission from ref. 33. Copyright 2018, American Association for the Advancement of Science.

2860 | *Chem. Soc. Rev.*, 2020, **49**, 2852–2868

This journal is © The Royal Society of Chemistry 2020

Fig. 12 (a) The general strategy: the nucleation rate and crystal growth were controlled by lowering the feeding rate to synthesise highly crystalline CTF-HUST-HC1 and CTF-HUST-HC2. (b) PXRD patterns of CTF-HUST-HC1 samples at different feeding rates, normalised at $2\theta = 38°$ for clarity. Reproduced with permission from ref. 34. Copyright 2019, Wiley-VCH.

Fig. 13 (a) The Lewis acid-catalysed deprotection–condensation protocol was used to form the Pc-PBBA COF. Reproduced with permission from ref. 35. Copyright 2010, Springer Nature. (b) Illustration of the reaction pathway towards BTD-COF. Reproduced with permission from ref. 36. Copyright 2013, Royal Society of Chemistry.

peak for CTF-HUST-HC1 at $2\theta = 7.4°$ exhibited a sharp reduction tendency with the decrease of the feeding rate of the aldehydes (Fig. 12b), reflecting the realisation of improved crystallinity by slowing down the monomer feeding rate. Although further lowering the feeding rates can form larger regular sheets as observed by SEM characterization, the loss of smoothness of the obtained sheets was observed at 10 μL min^{-1}, which indicates that an optimal feeding rate (30 μL min^{-1}) is important to control their morphology (both size and smoothness). These findings also confirmed the effective control of the nucleation rate and crystal growth by tuning the feeding rate of monomers. Furthermore, the initial temperature is another important parameter affecting the reaction rate. The BET surface area of the resulting CTFs at moderate initial temperature (100 °C) was higher than that obtained at higher temperature (150 °C). It is speculated that low temperature cannot meet the energy barrier of cyclisation, while if the temperature is too high it is impossible to control the nucleation rate to form big crystals. Therefore, a suitable feeding rate of monomers and an appropriate initial polymerization temperature are two key factors in controlling the nucleation rate and self-correction process to obtain highly ordered CTFs. Thanks to the efficient separation of photogenerated electron–hole pairs and charge transfer, the highly ordered CTF-HUST-HC1 exhibited superior performance on the photocatalytic removal of nitric oxide (NO) than the less crystalline counterparts and g-C$_3$N$_4$.

3.6 Protection of functional groups

In the conventional synthesis of boronic ester- or imine-linked COFs, multivariant free reactive groups (*e.g.*, boronic acid, catechol, amine and aldehyde) always suffer from easy oxidation, limited availability and poor solubility, which severely impede the development of COFs for diverse applications. To overcome these restrictions, a new method has been developed for the synthesis of boronate ester-linked COFs (Pc-PBBA COF) by direct condensation
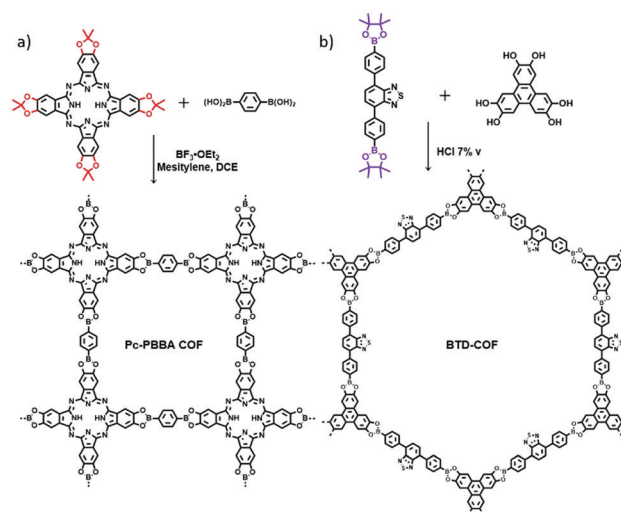
of acetonide-protected catechol and arylboronic acids (Fig. 13a) using Lewis acid (BBr$_3$) as a catalyst.[35] The protected catechol featured much enhanced stability and solubility. This approach exhibited wide generality and accessibility to complex boronate ester-linked COFs. Furthermore, a mechanistic study illustrated that the boronate ester formation rate depends on the dehydrative trimerization of boronic acids to boroxines. The formation of non-productive aryl boronic acid–BF$_3$ and ester hydrolysis are the most important steps in the COF formation under Lewis acid-catalysed conditions.

Similarly, another general protocol was employed by using pinacol-protected benzo[c][1,2,5]thiadiazole-4,7-diylbis(4,1-phenylene)diboronic acid (BTDBE) as the direct condensation monomer to react with catechol linkers (HHTP) for the synthesis of boronate ester-linked BTD-COF (Fig. 13b) through a two-step microwave synthesis procedure.[36] It is noteworthy that the corresponding boronate ester-linked BTD-COF could not be obtained by direct transesterification of BTDBE with HHTP in a one-pot manner. Utilisation of a boronate ester precursor as the starting material is a reliable approach to address the instability and insolubility of some free boronic acid monomers.

Most imine-linked COFs were synthesised by polycondensation of aldehydes and amines. However, aromatic aldehydes and amines are prone to oxidation and have low solubility. Hence, Li *et al.* also tried the functional group protection strategy toward imine COF synthesis. Three imine-linked COFs (LZU-20, 21 and 22) were synthesised using dimethyl acetal protected aldehyde monomers (Fig. 14a) with various amines *via* straightforward condensation reaction.[37] These dimethyl acetal precursors could be facilely prepared and featured higher solubility in common organic solvents. The generality of this approach was also confirmed by the synthesis of hydrazone-linked and azine-linked COFs.[37] On the other hand, the amines can also be protected by either benzophenone-imine[38,39] or *tert*-butyloxycarbonyl (Boc)[40]

This journal is © The Royal Society of Chemistry 2020

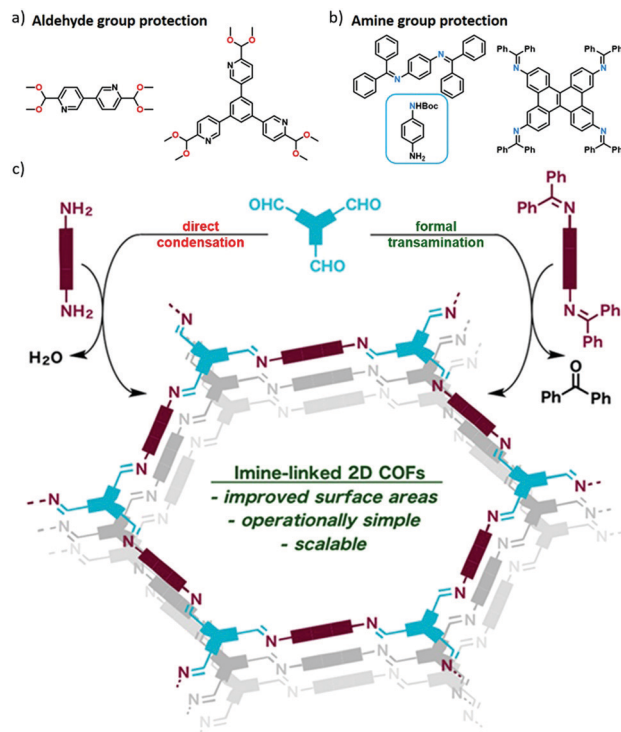*Chem. Soc. Rev.*, 2020, **49**, 2852–2868 | **2861**

Fig. 14 (a and b) Several representative protected aldehyde and amine monomers. (c) Comparison of the synthesis of imine-linked 2D COFs from polyfunctional aryl amine monomers (left) and the corresponding benzophenone imines (right). Reproduced with permission from ref. 38. Copyright 2017, American Chemical Society.

(Fig. 14b) and used as the monomers for imine-linked COF synthesis upon *in situ* deprotection. The *N*-aryl benzophenone imine monomers can be synthesised from the corresponding aryl amines with benzophenone using TiCl$_4$ as a catalyst,[38] or directly prepared *via* Buchwald–Hartwig coupling.[39] The imine- and β-ketoenamine-linked COFs using *N*-aryl benzophenone imines showed better crystallinity and higher surface areas than those of the counterparts synthesised using the corresponding unprotected aryl amines (Fig. 14c). The approach is amenable to both solvothermal and microwave irradiation syntheses. Another amine protection protocol is using *tert*-butyloxycarbonyl (Boc) as the protective group.[40] The Boc-protected amine can be deprotected *in situ*, thus resulting in stepwise nucleation and reduction of the imine condensation reaction rate, which further leads to the formation of well-distributed COF nanocrystals with woven structures.

3.7 Two-in-one strategy

Precise obeyance of the stoichiometry of the reactive sites may be beneficial to improving the solvent adaptability, reproducibility and crystallinity of COFs. We have recently developed a two-in-one strategy for facile synthesis of highly crystalline 2D imine-linked COFs with good solvent adaptability and reproducibility.[41] The basic concept is the integration of two different functional groups (reactive sites) into the same molecules. Generally, formyl and amino groups are indispensable for imine-linked COF synthesis but mostly distributed in two monomers. We elaborately designed

bifunctional monomers which simultaneously contain both formyl and amino groups. Thus, the conventional co-polycondensation of amines and aldehydes has been changed to the self-polycondensation of two-in-one bifunctional monomers. A unique feature of this strategy is that the bifunctional monomers possess equivalent formyl and amino groups, and thus the ideal stoichiometry can be strictly maintained throughout the polymerisation process. Such a system is ideal for reducing the dependency of reaction solvents. For example 1,6-bis(4-formyl-phenyl)-3,8-bis(4-aminophenyl)pyrene (BFBAPy) was explored for the successful preparation of the corresponding Py-COFs (Fig. 15a). Py-COFs with outstanding crystallinity and porosity (>1000 m^2 g^{-1}) were readily obtained in at least eight different common organic solvents such as dichloromethane (DCM), chloroform and tetrahydrofuran (THF), revealing their eminent solvent adaptability. Meanwhile, all the Py-COF samples synthesised under different conditions exhibited the same chemical compositions, comparable crystallinities and similar surface areas, which demonstrated the reproducibility of the two-in-one strategy for COF synthesis. Besides, Py-COF films with high crystallinity and tunable thickness could be easily prepared on various common or pre-modified substrates owing to their solvent adaptability. In contrast, the reported Py–Py COF with a similar structure to the Py-COF obtained by the conventional co-polycondensation method exhibited smaller surface areas and poor solvent adaptability. Py-COF films grown on ITO substrates with PEDOT/PSS coatings could serve as hole transporting layers for perovskite solar cells. Additionally, two new dual-pore COFs which cannot be constructed *via* a co-condensation method were further synthesised to demonstrate the versatility of this strategy. More recently, some new two-in-one building blocks with special catalytic sites were designed and synthesised. For example, two new two-in-one monomers with porphyrin[42] and benzoxazole[43] backbones were applied to construct the corresponding COFs. Crystalline 2D A$_2$B$_2$-Por-COFs (Fig. 15b) were easily synthesised in dichloromethane, chloroform and 1,2-dichloroethane, and all of these A$_2$B$_2$-Por-COFs exhibited large surface areas (>700 m^2 g^{-1}) and outstanding thermal and chemical stabilities. Benefiting from the photosensitivity and alkalinity of porphyrin free base, the A$_2$B$_2$-Por-COF was employed as an efficient heterogeneous catalyst for selective oxidation of sulfides and Knoevenagel condensation. Similarly, the benzoxazole BBO-COF (Fig. 15c) showcased excellent solvent adaptability which can be prepared in at least 11 different simplex solvents and exhibited preeminent crystallinity and large surface areas (>1000 m^2 g^{-1}). BBO-COF showed extraordinary chemical stability under corrosive conditions like aqueous 12 M HCl and 12 M NaOH solutions. It is worth mentioning that the crystallinity and porosity of BBO-COF can be maintained even after heating at 400 °C for 1 h or under visible light for 7 days. Thus, BBO-COF was applied to catalyse the oxidative hydroxylation of arylboronic acids under visible light with prominent catalytic activities.

The two-in-one strategy is unique in that it greatly simplifies the solvent screening process, and more importantly, it enables the synthesis of various COFs with high crystallinity and porosity in various solvents. The generality and versatility of the two-in-one
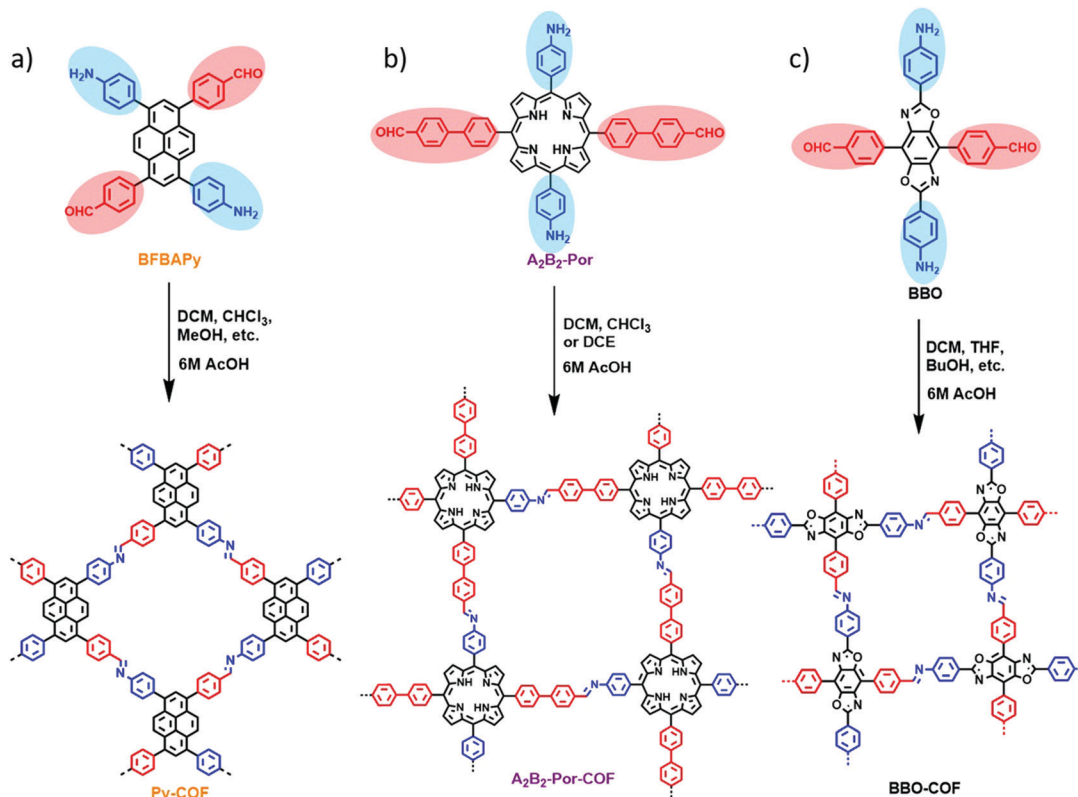
2862 | *Chem. Soc. Rev.*, 2020, **49**, 2852–2868

This journal is © The Royal Society of Chemistry 2020

Fig. 15 (a–c) A series of imine-linked COFs constructed by a "two-in-one" strategy. Reproduced with permission from ref. 41–43. Copyright 2019, American Chemical Society.

strategy were also verified by a series of different imine COFs facilely synthesised with reproducibility and high quality. We anticipate that this strategy can be extended to different synthetic techniques like chemical vapor deposition and interface-assisted synthesis of molecular frameworks.[41] Moreover, the two-in-one strategy is applicable for the synthesis of COFs with different building blocks and various linkages.

3.8 Novel COF film fabrication methods

As described above, most COFs are obtained as insoluble and unprocessable solids. It is a great challenge to incorporate these bulky COF powders into devices.[9] 3D printing technology is one of the effective post-processing approaches for COF powders and provides a facile method to fabricate designed multicomponent COF monoliths,[44] but there are more efficient methods for processing of COF powders into films for further applications. Therefore, to prepare substrate-supported COF films or free-standing COF films is an imperative and important research topic for realizing new applications of COFs. The size, thickness and orientation of COF films are highly interrelated to their functions and performance. To date, considerable efforts have been devoted towards the fabrication of COF films with single or few layers by either a bottom-up or top-down strategy.[9] In this section, we focus on new methods to highlight the recent progress in film fabrication.

Highly crystalline COF films on single-layer graphene (SLG) have been demonstrated *via* a bottom-up strategy under solvo-

thermal conditions.[11] There are many other reports of COF films developed on various substrates such as indium-doped tin oxide (ITO), fluorine-doped tin oxide (FTO), and Si/SiO₂ and platinum.[9] Unfortunately, there are many disadvantages for this solvothermal synthesis of COF films, including the inability to transfer films to target substrates, difficulties in scale up, low yields and a limited variety of substrates which can be compatible with the solvothermal conditions. Thus, the interfacial polymerization has attracted broad attention because it can be used to fabricate free standing COF films. It enables fabrication of films with variable sizes and tunable thickness and transfer of the films onto desired substrates for various applications. The free-standing films obtained by the interfacial polymerization have been demonstrated to be very promising for gas separation, sewage treatment and fuel cells.[9]

Besides this bottom-up strategy, another most applied method is the top-down exfoliation (either physically or chemically) of 2D COFs into COF nanosheets (CONs), resembling the delamination of graphite. For example, Banerjee *et al.* developed a simple yet effective mechanical method for delamination of 2D imine COFs into CONs using a mortar and pestle system or ball milling.[13] The thickness of the obtained nanosheets can be down to only a few nanometres, but unfortunately, they exhibited weak crystallinity and no preferred orientation.

Besides the traditional mechanical exfoliation method, chemically assisted exfoliation has been developed to delaminate 2D bulky COFs into few-layer COF nanosheets,[45–47] which is effective in

This journal is © The Royal Society of Chemistry 2020

Chem. Soc. Rev., 2020, **49**, 2852–2868 | **2863**

obtaining few-layer or even single-layer 2D polymers. In 2016, the Diels–Alder cycloaddition reaction was first utilized to fabricate free-standing ultrathin COF nanosheets. Upon cycloaddition with *N*-hexylmaleimide, the formed pendant hexyl groups disrupted the π–π stacking of the COF layers, and the planarity of the anthracene units in DaTp-COF was broken to afford uniform, free-standing nanosheets.[45] Recently, a new chemical exfoliation strategy has been developed to afford few-layer E-TFPB-COF and E-TFPB-COF/MnO$_2$ composites for efficient energy storage.[46] The bulky TFPB-COF could be stripped into few-layered nanosheet structures by the strong oxidants KMnO$_4$ and HClO$_4$ (Fig. 16a). The resulting few-layer nanosheets (Fig. 16b–d) are beneficial for the transport of ions/electrons with fast kinetics and furnish new accessible redox-active sites from the π electrons of the benzene rings for lithium storage. As a consequence, these exfoliated E-TFPB-COF/MnO$_2$ composites and E-TFPB-COF present large reversible capacities and excellent cycling performances (1359 and 968 mA h g^{-1}, respectively, after 300 cycles). In contrast, the bulky TFPB-COF merely exhibited a moderate capacity of 126 mA h g^{-1} after 300 cycles. These results demonstrate that the chemical exfoliation strategy may be a valid and efficient method to delaminate COFs for energy storage.

Very recently, a scalable chemically assisted acid exfoliation approach has been utilised to delaminate a series of 2D imine COF powders and sequentially cast crystalline COF thin films with large area and tunable thickness.[47] Excess trifluoroacetic acid (TFA) was employed to protonate the imine COFs and accelerate their dispersion in organic solvents due to the charge repulsion effect. The well dispersed suspensions were prepared by stirring the bulky COF powders in a mixture of acetonitrile, tetrahydrofuran, and TFA (7/3/2, v/v/v) overnight (Fig. 16e). After acid exfoliation treatments, the exfoliated samples maintained the chemical composition but with largely decreased surface areas and crystallinities probably due to the disordered stacking of the protonated COF sheets. Interestingly, highly crystalline and continuous COF films can be readily formed by depositing the exfoliated suspensions onto a silicon wafer substrate upon gradual evaporation of the solvents. More importantly, the films can be detached from the substrate, affording free-standing films which usually cannot be obtained by the conventional *in situ* solvothermal growth. The thickness of the films can be directly tuned by varying the concentration of the exfoliated COF suspension or casting procedures such as spin-coating and drop-casting. This acid induced exfoliation may furnish a versatile and powerful strategy to produce large-scale imine-linked COF films with high crystallinity, porosity and controlled size/thickness for further device applications.

In addition to the exfoliation methods, the above-mentioned colloidal COF nanoparticles prepared in acetonitrile[33] provide new opportunities for free-standing films *via* subsequent solution-casting protocols.[48] Such solution-cast COF films from colloidal COF nanoparticles retained the crystallinity and pore size in agreement with the powders. Interestingly, they exhibited a preferred orientation opposite to those of the films prepared by *in situ* solvothermal growth on substrates (Fig. 17a).

Besides, the interfacial synthesis method has drawn much attention to prepare free-standing COF films. A two-dimensional
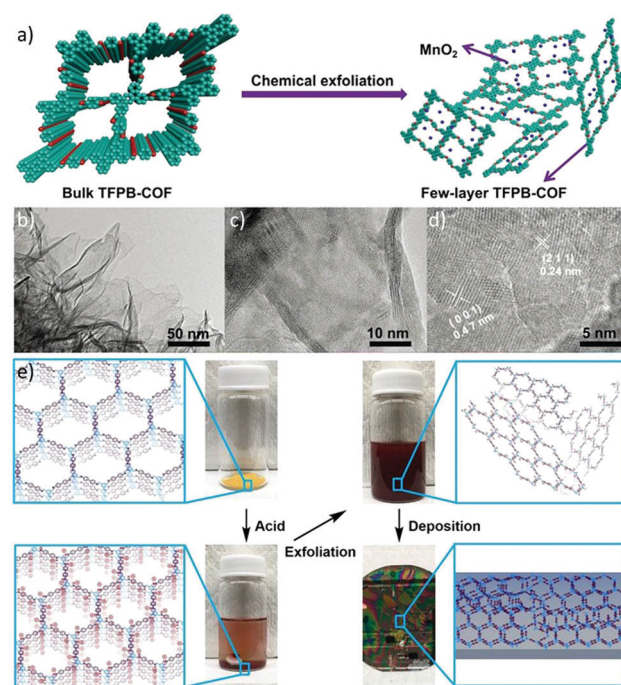

Fig. 16 (a) Schematic illustration for the chemical exfoliation of TFPB-COF. (b–d) HRTEM images of few-layer E-TFPB-COF/MnO$_2$. Reproduced with permission from ref. 46. Copyright 2019, Wiley-VCH. (e) Overview of acid exfoliation and film casting procedures. Protonation of imine-linked COF powders results in electrostatic repulsion between adjacent layers, which induces rapid exfoliation of the powders into thin nanosheets upon stirring. Suspensions of exfoliated COF nanosheets were deposited onto substrates and formed thin, crystalline COF films upon drying. Reproduced with permission from ref. 47. Copyright 2020, Wiley-VCH.
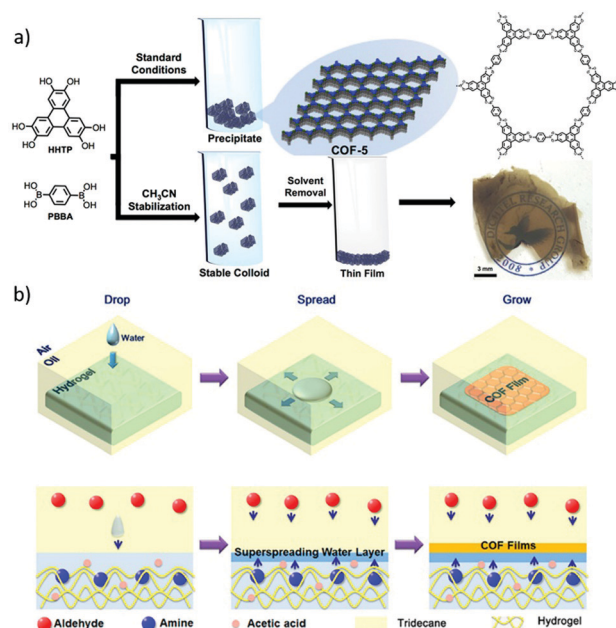

Fig. 17 (a) Solution casting of colloids produces a coherent, free-standing COF film. Reproduced with permission from ref. 48. Copyright 2017, American Chemical Society. (b) Schematic illustration for the fabrication of COF thin films at hydrogel surfaces based on the confined super-spreading water layers under oil. Reproduced with permission from ref. 50. Copyright 2018, American Chemical Society.

covalent organic monolayer has been fabricated *via* the Langmuir–Blodgett method.[49] Aromatic polyimine monolayers in millimeter size can be obtained after the polymerization of dialdehydes and triamines which occurs at the air/water interface. This work presents the first example of freestanding polyimine monolayers and facilitates the exploration of the corresponding 2D conjugated polymers. Recently, a confined synthesis strategy has been developed for synthesis of free-standing COF films at an oil/water/hydrogel interface.[50] A swollen hydrogel with amine monomers was immersed in an oil phase (tridecane) with the aldehyde monomer, followed by dropping water droplets on the hydrogel to form thin superspreading water layers. Then, these reactants diffused into the water layers to form the corresponding COF thin films (Fig. 17b). The resulting COF films can be transferred and further characterised. Large area, crystalline and oriented free-standing COF thin films with a homogeneous topography and controllable thicknesses from 4 to 150 nm were obtained. Importantly, the COF films exhibited a Young's modulus of 25.9 ± 0.6 GPa. This strategy on hydrogel interfaces can be expanded to the growth of a crystalline ZIF-8 thin film, suggesting its generality.

Free-standing, crystalline and few-layer 2D polyimide (2DPI) and 2D polyamide (2DPA) films have recently been demonstrated by interfacial synthesis on the water surface.[51] Monolayers of surfactants such as sodium (9Z)-octadec-9-en-1-yl sulfate (sodium oleyl sulphate, SOS) and octadecanoic acid (stearic acid, SA) were employed to assist the synthesis of these films due to their significant effect on the pre-organisation of amine monomer *via* electrostatic interaction. A general protocol for the fabrication of these few-layer films is summarised as follows: a monolayer of surfactant (SOS) on the water surface was prepared, followed by the addition of amine monomer into water (Fig. 18a). Next, the anhydride monomer was injected into the water and the mixture was maintained at 20 °C under ambient conditions for 7 days. The reaction time was related to the surfactant; few-layer 2DPA could be formed overnight when SA was utilised (Fig. 18b). 2DPI with a thickness of ∼2 nm and an average crystal domain size of ∼3.5 μm^2 and 2DPA with a thickness of ∼10 nm and an average crystal domain size of ∼0.3 μm^2 were obtained. Both 2DPI and 2DPA synthesised using SOS surfactant exhibited a face-on orientation. In contrast, 2DPA synthesised *via* the SA monolayers exhibited an edge-on orientation because the amine monomer could be vertically anchored by SA.

Fabrication of large-area and high-quality thin 2D films and further assembly to form new van der Waals heterostructures greatly enrich the chemical diversity and functionality of 2D materials. Recently, a new interfacial synthesis strategy, laminar assembly polymerization (LAP) at a sharp pentane/water interface (Fig. 19), has been reported.[52] This technique enables scalable synthesis and facile processing of large-area 2D polymers and is compatible with various molecular monomers for the formation of monolayer COFs or MOFs (Fig. 19a). Different from the traditional liquid–liquid interfacial synthesis methods, the LAP method involves three phases: injection, self-assembly and polymerisation. Firstly, the monomers were injected at the
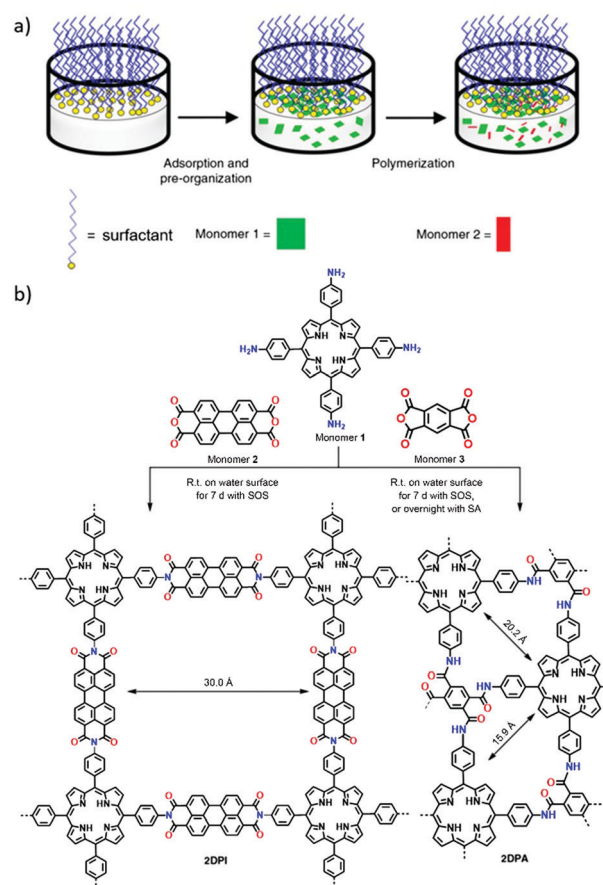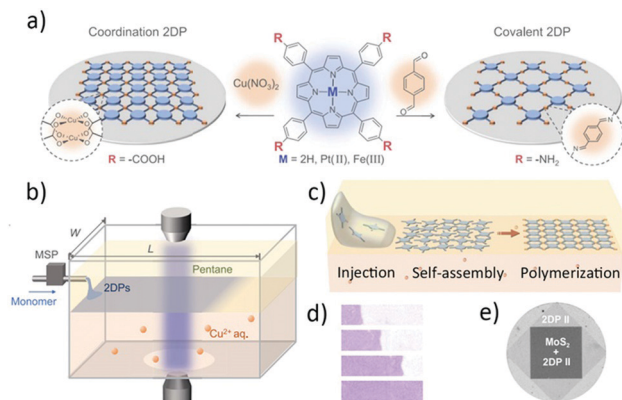

Fig. 18 (a) Schematic drawing of the synthetic procedure for 2D polymers on the water surface assisted by a surfactant monolayer. (b) A reaction scheme illustrating the synthesis of 2DPI and 2DPA *via* condensation reactions, with the assistance of surfactant monolayers on the water surface. Reproduced with permission from ref. 51. Copyright 2019, Springer Nature.

edge of the reactor and directly transported onto the sharp pentane/water interface by a continuous stream of carrier solution through the pentane layer. Subsequently, the delivered porphyrin-based monomers self-assembled at the interface owing to their amphiphilicity and spread, but being restricted by the longer sidewalls. This process produced laminar flow of the monomers away from the injection region and led to a continuous monolayer assembly. Finally, the assembled monomers gradually polymerised *via* the reaction with the reagents dissolved in water (Fig. 19b–d). The advantages of the LAP synthesis are that it not only produces large area monolayer 2D films, but is also compatible with a large number of patterning and transfer techniques. Furthermore, Zhong *et al.* integrated the 2DP monolayer with molybdenum disulfide for the fabrication of hybrid superlattices, which exhibited excellent electrical properties (Fig. 19e).

A buffering interlayer interface (BII) method has been developed for monomers with limited solubility to form high-quality 2D COF nanosheets.[53] DCM (A) and DCM-DMF (B) mixed solvents are selected as two miscible organic solvents which are able to dissolve 1,3,5-triformylphloroglucinol (TFP) and dihydroxybenzidine (DHBD). Acetic acid (C) is chosen as both a catalyst and a buffer
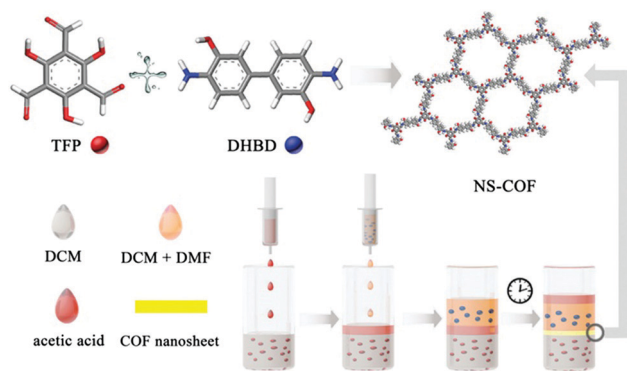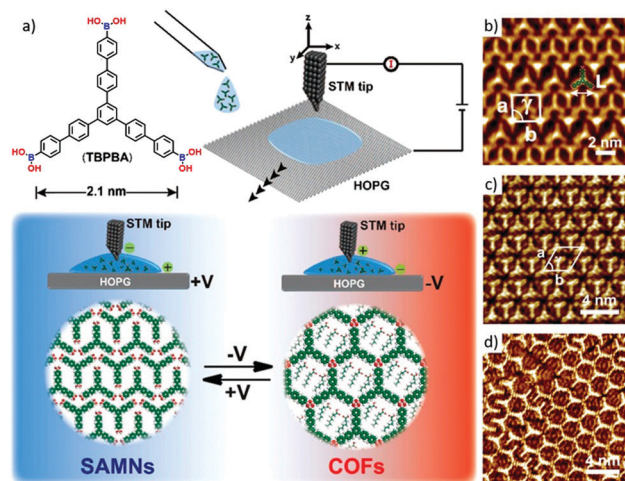
This journal is © The Royal Society of Chemistry 2020

Chem. Soc. Rev., 2020, **49**, 2852–2868 | **2865**

Fig. 19 (a) Schematic illustration of monolayer 2DPs and the corresponding chemical structures of the molecular precursors. (b) Schematic view of a LAP reactor and *in situ* optical characterization apparatus. MSP, microsyringe pump. (c) Schematic presentation of the LAP synthesis that involves three phases. (d) False-colour images of a 2DP I film at four different stages during growth. (e) Optical transmission image of a 2DP II/MoS$_2$ heterostructure on fused silica taken at a wavelength of 405 nm. Reproduced with permission from ref. 52. Copyright 2019, American Association for the Advancement of Science.

Fig. 21 (a) Schematic illustration of the electric-field-induced reversible transformation between self-assembled molecular networks (SAMNs) and covalent organic frameworks (COFs); and (b–d) high-resolution STM images of the self-assembled phases A, A′ and B at the 1-octanoic acid/HOPG interface. Reproduced with permission from ref. 54. Copyright 2019, American Chemical Society.

solvent. The addition order of the three solvents is A + C + B to form a sandwich type organic solvent system (Fig. 20). The buffering solvent (C) can postpone the diffusion of B to the surface of A which is conducive to the formation of high-quality COF nanosheets with a super-large (>200 μm^2) and smooth surface. The obtained nanosheets were stable and showed sensitive detection and selective sorption of UO_2^{2+}. This approach also showed applicability to some other diamine monomers.[53]

Taking advantage of the dynamic nature of boronic ester linkage, the reversible transformation between self-assembled diboronic acid supramolecular networks and 2D COFs can be regulated upon exposure to external electric-field stimuli *via* STM (Fig. 21a).[54] Interestingly, local noncovalent phases (A, A′, Fig. 21b and c) that existed under a positive sample bias can be converted to regular porous phase B (Fig. 21d) by changing the polarity of the electric field to a negative bias. The local concentration of water at the 1-octanoic acid/HOPG interface

had a clear impact on the switching process. The surface's switching behaviour mediated by the electric field could be expanded to multicomponent systems and other linkages.

In addition to the methods mentioned above, a novel electrophoretic deposition (EPD) approach has been exploited to fabricate large area COF films.[55] This technique is easy to implement: two conductive substrates as electrodes were submerged into a nonconducting COF particle suspension and COF nanoparticles
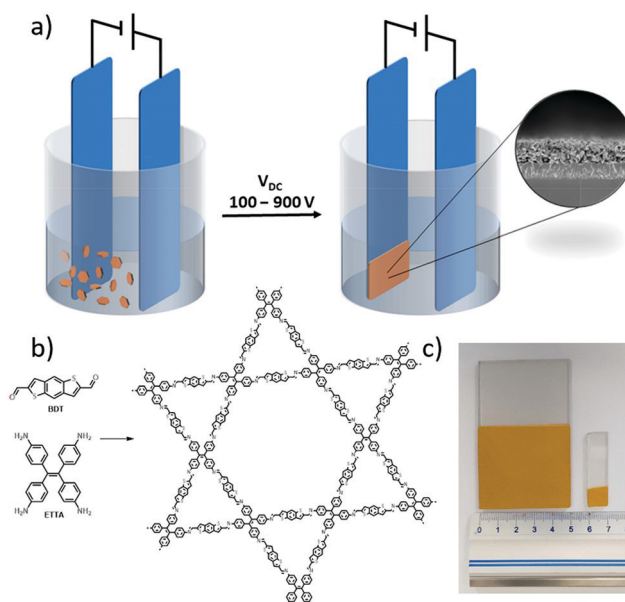
Fig. 22 (a) Schematic presentation of an EPD setup with a typical cross-sectional SEM image of the COF film shown in the inset. (b) Synthetic approach for BDT-ETTA-COF. (c) Photograph of an EPD of BDT-ETTA-COF on a 5 cm × 5 cm electrode area as well as a 1 cm × 1 cm film. Both depositions were carried out on FTO at 900 V for 2 min. Reproduced with permission from ref. 55. Copyright 2019, American Chemical Society.

Fig. 20 Schematic representation of the preparation process involving a buffering interlayer in growing 2D COF nanosheets. Reproduced with permission from ref. 53. Copyright 2018, Royal Society of Chemistry.

could migrate to the surface of the electrode to form COF films when an external electric field (100 to 900 V cm^{-1}) was applied (Fig. 22a). Large-area films up to 25 cm^2 could be obtained within 2 minutes by this approach (Fig. 22c). The EPD method is applicable to fabricating films of some representative 2D and 3D COFs with different kinds of linkages such as COF-5 (boronate-linked),[2] COF-300[6] and BDT-ETTA-COF[55] (imine-linked, Fig. 22b). All these films were coated on the positively charged electrode, indicating that COF particles bear intrinsic negative surface charges. The thicknesses of the films could be tuned from 400 nm to 24 μm by adjusting the deposition time, particle concentration and electrode potential. Furthermore, composite films consisting of mixed COF particles can also be directly prepared by this EPD approach.

The progress in developing the above strategies has greatly enriched the approaches to fabricating high quality COF films either on substrates or as free-standing films to enable and expand the application of COFs. Moreover, recent progress in graphene and 2D inorganic materials would inspire the development of COF films.

4. Conclusion and perspectives

In this tutorial review, we have summarised the recent key progress in the synthesis of COFs by highlighting new strategies, which are distinct from conventional solvothermal and ionothermal syntheses. The rapid development over the past 15 years in COF chemistry undoubtedly has demonstrated that COFs have emerged as a promising molecular platform for structural design and tailored functional exploration. In recent years, COFs have been demonstrated to be utilized in many fields such as mass transport, chiral catalysis, and semiconductors,[1] which benefit from their regular open nanochannels, ordered π-arrays and designable structures. It is noteworthy that the first fully conjugated and crystalline sp^{2}c-COF can form a ferromagnetic state below 10 K upon oxidation by iodine, while such magnetic features are hardly realized in 1D conjugated polymers or their conventional porous material counterparts.[1] However, there are still key fundamental issues to be addressed for challenging practical applications.

Precise control of primary and high-order structures and structural analysis represent the most important issues that need to be addressed. A reliable method for preparation of single crystals, especially for 2D COFs, is of critical importance. The reproducibility and quality control of COF crystallites and films are also crucial for their applications. Large-scale synthesis should be settled and realised before their practical applications. Thus, efficient synthesis of monomers and scalable techniques for COF preparation are highly desired.

Unique functions and applications of COFs which are inaccessible to other porous counterparts like MOFs, zeolites, cages and porous silica should be an important aspect worthy of further exploration. Owing to the abundant and highly ordered π-conjugated units in the skeletons, further exploration of COFs toward electronics, optoelectronics and spintronics is an interesting subject. In relation to this, the structure–property correlations are still unclear for most COFs. For example, structural correlations

with the properties of monolayers, a few layers and bulky frameworks have not been well explored. These relationships are important for disclosing the inherent properties of COFs.

There are great demands in the separation industry which needs stable and highly porous membranes with controllable and ordered open channels as they offer an efficient and energy-saving purification. Although membranes based on MOFs and zeolites have been developed, the combination of stability, design flexibility and porosity endows COF-based films and membranes with great potential in industrial separation processes. Materials engineering and processing will be another challenging subject for large-scale applications.

The COF field offers a molecular platform in which chemistry, physics and materials science play together to disclose the mystery in these ordered organic lattices, which are hardly accessible to self-assemblies and single crystals of organic systems. With the development of single crystals and well-defined films, the physics underlying the property and functions (*e.g.* charge carrier and spin polarized transport) will be an important topic. The collaboration between chemistry, physics, materials science and engineering will definitely disclose a full picture of the COF field, which will offer invaluable solutions to environmental, resource and energy issues.

Conflicts of interest

There are no conflicts to declare.

Acknowledgements

Notes and references

1 K. Geng, T. He, R. Liu, K. T. Tan, Z. Li, S. Tao, Y. Gong, Q. Jiang and D. Jiang, *Chem. Rev.*, 2020, DOI: 10.1021/acs.chemrev.9b00550.

2 A. P. Côté, A. I. Benin, N. W. Ockwig, M. O'Keeffe, A. J. Matzger and O. M. Yaghi, *Science*, 2005, **310**, 1166–1170.

3 P. Kuhn, M. Antonietti and A. Thomas, *Angew. Chem., Int. Ed.*, 2008, **47**, 3450–3453.

4 X. Zhuang, W. Zhao, F. Zhang, Y. Cao, F. Liu, S. Bi and X. Feng, *Polym. Chem.*, 2016, **7**, 4176–4181.

5 E. Jin, M. Asada, Q. Xu, S. Dalapati, M. Addicoat, M. A. Brady, H. Xu, T. Nakamura, T. Heine, Q. Chen and D. Jiang, *Science*, 2017, **357**, 673–676.

6 T. Ma, E. A. Kapustin, S. X. Yin, L. Liang, Z. Zhou, J. Niu, L.-H. Li, Y. Wang, J. Su, J. Li, X. Wang, W. D. Wang, W. Wang, J. Sun and O. M. Yaghi, *Science*, 2018, **361**, 48–52.

7 Y. Jin, Y. Hu and W. Zhang, *Nat. Rev. Chem.*, 2017, **1**, 0056.

8 B. J. Smith and W. R. Dichtel, *J. Am. Chem. Soc.*, 2014, **136**, 8783–8789.

This journal is © The Royal Society of Chemistry 2020

Chem. Soc. Rev., 2020, **49**, 2852–2868 | **2867**

9 H. Wang, Z. Zeng, P. Xu, L. Li, G. Zeng, R. Xiao, Z. Tang, D. Huang, L. Tang, C. Lai, D. Jiang, Y. Liu, H. Yi, L. Qin, S. Ye, X. Ren and W. Tang, *Chem. Soc. Rev.*, 2019, **48**, 488–516.

10 S. Kandambeth, K. Dey and R. Banerjee, *J. Am. Chem. Soc.*, 2019, **141**, 1807–1822.

11 J. W. Colson, A. R. Woll, A. Mukherjee, M. P. Levendorf, E. L. Spitler, V. B. Shields, M. G. Spencer, J. Park and W. R. Dichtel, *Science*, 2011, **332**, 228–231.

12 N. L. Campbell, R. Clowes, L. K. Ritchie and A. I. Cooper, *Chem. Mater.*, 2009, **21**, 204–206.

13 B. P. Biswal, S. Chandra, S. Kandambeth, B. Lukose, T. Heine and R. Banerjee, *J. Am. Chem. Soc.*, 2013, **135**, 5328–5331.

14 Y. Peng, G. Xu, Z. Hu, Y. Cheng, C. Chi, D. Yuan, H. Cheng and D. Zhao, *ACS Appl. Mater. Interfaces*, 2016, **8**, 18505–18512.

15 Y. Zeng, R. Zou, Z. Luo, H. Zhang, X. Yao, X. Ma, R. Zou and Y. Zhao, *J. Am. Chem. Soc.*, 2015, **137**, 1020–1023.

16 X. Chen, M. Addicoat, E. Jin, H. Xu, T. Hayashi, F. Xu, N. Huang, S. Irle and D. Jiang, *Sci. Rep.*, 2015, **5**, 14650.

17 J.-Y. Yue, Y.-P. Mo, S.-Y. Li, W.-L. Dong, T. Chen and D. Wang, *Chem. Sci.*, 2017, **8**, 2169–2174.

18 N. Huang, L. Zhai, D. E. Coupry, M. Addicoat, K. Okushita, K. Nishimura, T. Heine and D. Jiang, *Nat. Commun.*, 2016, **7**, 12325.

19 Z.-F. Pang, S.-Q. Xu, T.-Y. Zhou, R.-R. Liang, T.-G. Zhan and X. Zhao, *J. Am. Chem. Soc.*, 2016, **138**, 4710–4713.

20 P.-L. Wang, S.-Y. Ding, Z.-C. Zhang, Z.-P. Wang and W. Wang, *J. Am. Chem. Soc.*, 2019, **141**, 18004–18008.

21 P.-F. Wei, M.-Z. Qi, Z.-P. Wang, S.-Y. Ding, W. Yu, Q. Liu, L.-K. Wang, H.-Z. Wang, W.-K. An and W. Wang, *J. Am. Chem. Soc.*, 2018, **140**, 4623–4631.

22 X. Li, C. Zhang, S. Cai, X. Lei, V. Altoe, F. Hong, J. J. Urban, J. Ciston, E. M. Chan and Y. Liu, *Nat. Commun.*, 2018, **9**, 2998.

23 S. J. Lyle, T. M. O. Popp, P. J. Waller, X. Pei, J. A. Reimer and O. M. Yaghi, *J. Am. Chem. Soc.*, 2019, **141**, 11253–11258.

24 J.-M. Seo, H.-J. Noh, H. Y. Jeong and J.-B. Baek, *J. Am. Chem. Soc.*, 2019, **141**, 11786–11790.

25 X.-T. Li, J. Zou, T.-H. Wang, H.-C. Ma, G.-J. Chen and Y.-B. Dong, *J. Am. Chem. Soc.*, 2020, **142**, 6521–6526.

26 J. Tan, S. Namuangruk, W. Kong, N. Kungwan, J. Guo and C. Wang, *Angew. Chem., Int. Ed.*, 2016, **55**, 13979–13984.

27 M. Matsumoto, R. R. Dasari, W. Ji, C. H. Feriante, T. C. Parker, S. R. Marder and W. R. Dichtel, *J. Am. Chem. Soc.*, 2017, **139**, 4999–5002.

28 S. Karak, S. Kandambeth, B. P. Biswal, H. S. Sasmal, S. Kumar, P. Pachfule and R. Banerjee, *J. Am. Chem. Soc.*, 2017, **139**, 1856–1862.

29 S. Karak, S. Kumar, P. Pachfule and R. Banerjee, *J. Am. Chem. Soc.*, 2018, **140**, 5138–5145.

30 C. Qian, Q.-Y. Qi, G.-F. Jiang, F.-Z. Cui, Y. Tian and X. Zhao, *J. Am. Chem. Soc.*, 2017, **139**, 6736–6743.

31 Y. Zhai, G. Liu, F. Jin, Y. Zhang, X. Gong, Z. Miao, J. Li, M. Zhang, Y. Cui, L. Zhang, Y. Liu, H. Zhang, Y. Zhao and Y. Zeng, *Angew. Chem., Int. Ed.*, 2019, **58**, 17679–17683.

32 S. Wang, Z. Zhang, H. Zhang, A. G. Rajan, N. Xu, Y. Yang, Y. Zeng, P. Liu, X. Zhang, Q. Mao, Y. He, J. Zhao, B.-G. Li, M. S. Strano and W.-J. Wang, *Matter*, 2019, **1**, 1592–1605.

33 A. M. Evans, L. R. Parent, N. C. Flanders, R. P. Bisbey, E. Vitaku, M. S. Kirschner, R. D. Schaller, L. X. Chen, N. C. Gianneschi and W. R. Dichtel, *Science*, 2018, **361**, 52–57.

34 M. Liu, K. Jiang, X. Ding, S. Wang, C. Zhang, J. Liu, Z. Zhan, G. Cheng, B. Li, H. Chen, S. Jin and B. Tan, *Adv. Mater.*, 2019, **31**, 1807865.

35 E. L. Spitler and W. R. Dichtel, *Nat. Chem.*, 2010, **2**, 672–677.

36 M. Dogru, A. Sonnauer, S. Zimdars, M. Döblinger, P. Knochel and T. Bein, *CrystEngComm*, 2013, **15**, 1500–1502.

37 Z.-J. Li, S.-Y. Ding, H.-D. Xue, W. Cao and W. Wang, *Chem. Commun.*, 2016, **52**, 7217–7220.

38 E. Vitaku and W. R. Dichtel, *J. Am. Chem. Soc.*, 2017, **139**, 12911–12914.

39 Z. Xie, B. Wang, Z. Yang, X. Yang, G. Xing, Y. Zhang and L. Chen, *Angew. Chem., Int. Ed.*, 2019, **58**, 15742–15746.

40 Y. Zhao, L. Guo, F. Gándara, Y. Ma, Z. Liu, C. Zhu, H. Lyu, C. A. Trickett, E. A. Kapustin, O. Terasaki and O. M. Yaghi, *J. Am. Chem. Soc.*, 2017, **139**, 13166–13172.

41 Y. Li, Q. Chen, T. Xu, Z. Xie, J. Liu, X. Yu, S. Ma, T. Qin and L. Chen, *J. Am. Chem. Soc.*, 2019, **141**, 13822–13828.

42 W. Hao, D. Chen, Y. Li, Z. Yang, G. Xing, J. Li and L. Chen, *Chem. Mater.*, 2019, **31**, 8100–8105.

43 X. Yan, H. Liu, Y. Li, W. Chen, T. Zhang, Z. Zhao, G. Xing and L. Chen, *Macromolecules*, 2019, **52**, 7977–7983.

44 M. Zhang, L. Li, Q. Lin, M. Tang, Y. Wu and C. Ke, *J. Am. Chem. Soc.*, 2019, **141**, 5154–5158.

45 M. A. Khayum, S. Kandambeth, S. Mitra, S. B. Nair, A. Das, S. S. Nagane, R. Mukherjee and R. Banerjee, *Angew. Chem., Int. Ed.*, 2016, **55**, 15604–15608.

46 X. Chen, Y. Li, L. Wang, Y. Xu, A. Nie, Q. Li, F. Wu, W. Sun, X. Zhang, R. Vajtai, P. M. Ajayan, L. Chen and Y. Wang, *Adv. Mater.*, 2019, **31**, 1901640.

47 D. W. Burke, C. Sun, I. Castano, N. C. Flanders, A. M. Evans, E. Vitaku, D. C. McLeod, R. H. Lambeth, L. X. Chen, N. C. Gianneschi and W. R. Dichtel, *Angew. Chem., Int. Ed.*, 2020, **59**, 5165–5171.

48 B. J. Smith, L. R. Parent, A. C. Overholts, P. A. Beaucage, R. P. Bisbey, A. D. Chavez, N. Hwang, C. Park, A. M. Evans, N. C. Gianneschi and W. R. Dichtel, *ACS Cent. Sci.*, 2017, **3**, 58–65.

49 W. Dai, F. Shao, J. Szczerbiński, R. McCaffrey, R. Zenobi, Y. Jin, A. D. Schlîter and W. Zhang, *Angew. Chem., Int. Ed.*, 2016, **55**, 213–217.

50 Q. Hao, C. Zhao, B. Sun, C. Lu, J. Liu, M. Liu, L.-J. Wan and D. Wang, *J. Am. Chem. Soc.*, 2018, **140**, 12152–12158.

51 K. Liu, H. Qi, R. Dong, R. Shivhare, M. Addicoat, T. Zhang, H. Sahabudeen, T. Heine, S. Mannsfeld, U. Kaiser, Z. Zheng and X. Feng, *Nat. Chem.*, 2019, **11**, 994–1000.

52 Y. Zhong, B. Cheng, C. Park, A. Ray, S. Brown, F. Mujid, J.-U. Lee, H. Zhou, J. Suh, K.-H. Lee, A. J. Mannix, K. Kang, S. J. Sibener, D. A. Muller and J. Park, *Science*, 2019, **366**, 1379–1384.

53 Y. Li, M. Zhang, X. Guo, R. Wen, X. Li, X. Li, S. Li and L. Ma, *Nanoscale Horiz.*, 2018, **3**, 205–212.

54 Z.-F. Cai, G. Zhan, L. Daukiya, S. Eyley, W. Thielemans, K. Severin and S. DeFeyter, *J. Am. Chem. Soc.*, 2019, **141**, 11404–11408.

55 J. M. Rotter, S. Weinberger, J. Kampmann, T. Sick, M. Shalom, T. Bein and D. D. Medina, *Chem. Mater.*, 2019, **31**, 10008–10016.

2868 | *Chem. Soc. Rev.*, 2020, **49**, 2852–2868

This journal is © The Royal Society of Chemistry 2020